FILING SUBJECTS:

1. Steel, Physical and Mechanical Properties
2. Fracture Toughness
3. Rocket Motor Cases

METALLURGICAL ASPECTS OF FRACTURE AT HIGH STRENGTH LEVEL

Interim Technical Report

Prepared by

Walter A. Backofen

and

Merrill L. Ebner
Massachusetts Institute of Technology

March 1962

Frank Larson
Technical Advisor
Watertown Arsenal Laboratories
Watertown, Massachusetts

FILING SUBJECTS:

1. Steel, Physical and Mechanical Properties
2. Fracture Toughness
3. Rocket Motor Cases

METALLURGICAL ASPECTS OF FRACTURE AT HIGH STRENGTH LEVEL

Interim Technical Report

Prepared by

Walter A. Backofen

and

Merrill L. Ebner
Massachusetts Institute of Technology

March 1962

Frank Larson
Technical Advisor
Watertown Arsenal Laboratories
Watertown, Massachusetts

ABSTRACT

Part 1: Fracture Toughness of Hardened and Tempered AISI 4340 Sheet

The fracture toughness, K_c, of quenched and tempered sheet specimens of air-melted and cross-rolled AISI 4340 was measured by procedures basically in accordance with those recommended by the special ASTM Committee on Fracture Testing. Fracture toughness, K_c, was obtained from the elastic analysis of Irwin, with and without the plastic-zone correction, and by the elastic-plastic analysis of McClintock. The two values calculated from the Irwin analysis are essentially the same for specimens tempered below 400°F, but without correction values are 15% lower for specimens tempered at 700°F. K_c values calculated according to McClintock agree within 20% with the corrected Irwin values for specimens tempered between 500°F and 800°F.

Comparison of the K_c values with those of Rawe indicate that K_c for AISI 4340 is very sensitive to processing history. Extensive splitting, or delamination, along the plane of the sheet was observed in all fractures. It is suggested that this delamination, which is an event related to processing history, might contribute to low plane-strain fracture toughness and high toughness-transition temperature.

Part 2: Effect of Austenitizing Temperature on Fracture Mode of AISI 4340

Face-notched specimens of AISI 4340 were austenitized at 1550°F or 2300°F, quenched, refrigerated, tempered and broken in impact bending. The character of the fracture surfaces was observed in relationship to austenitizing temperature, tempering temperature, and testing temperature. When fracture did not occur along prior austenite grain boundaries, the surface appeared rougher (presumably associated with greater fracture toughness) for the larger grained material austenitized at 2300°F, regardless of the tempering or testing temperature. Preliminary fracture-toughness measurements agree with these fractographic observations.

TABLE OF CONTENTS

LIST OF ILLUSTRATIONS

LIST OF TABLES

PART 1: FRACTURE TOUGHNESS OF HARDENED AND TEMPERED AISI 4340 SHEET

I. INTRODUCTION

The well-known need in missile technology for the highest practical strength-weight ratio has required the use of high-strength steels in a lightly tempered, notch-sensitive condition. One consequence of such applications has been a certain amount of failure in motor casings by rapid propagation of small flaws undetected in final inspection. The mechanics of crack propagation have developed in the last decade into a useful tool for studying notch sensitivity. After the first analysis by Griffith,[1] Orowan[2] and Irwin[3] suggested that the basic concept could be applied to describe the propagation of cracks in large steel structures. The formulation of Irwin, in which the energy term in the Griffith equation is deduced from the elastic stress distribution at instability, has proven especially valuable.

The fracture toughness measured with notched sheet specimens of high-strength steel is dependent on such testing variables as the thickness of the sample and on the testing temperature. For a given composition, it is also dependent on processing history. Differences in microstructure, for example, resulting from different melting and rolling practices may have important effects on fracture toughness. In this connection, steels produced by consutrode and vacuum melting generally possess higher toughness and higher notch strength than the same steels when air melted, as indicated in Table I-1.[5] Unidirectional solidification of the starting ingot may also yield material with greater fracture toughness, since freezing in this fashion has been found to increase markedly the reduction of area in tension of AISI 4330 and 4340 steels.[6] Reduced microporosity and inclusion content and improved chemical homogeniety are identified with such improvement through control of melting practice. Still other evidence establishes the effect of rolling history, in particular the large differences between longitudinal and transverse properties of unidirectionally rolled sheet[5] compared to the far more isotropic fracture toughness in specimens from the plane of sheet that has been produced by cross-rolling.

The work being reported was the initial phase in a study of the effect of processing history on fracture toughness. It was necessary that detailed attention be paid to the problems of measuring the fracture toughness of sheet material, and this is the principal subject discussed here. For determination of the fracture toughness of sheet materials, test procedures have been recommended by the ASTM based on the Irwin point of view.[4] These specifications are most helpful in fixing specimen dimensions and notch sharpness and were followed in the present work with some few exceptions, which are noted.

TABLE I-1

EFFECT OF MELTING PRACTICE ON FRACTURE TOUGHNESS

	AMS 6434	AISI 4340	Tricent (300M)	Air Steel X-200	H-11	Unimach II
Air Melted	159*	141	99	67	98	117
Vacuum Induction Melted	107	172	--	227	--	187
Consutrode	261	247	143	157	125	176

* Average fracture toughness (K_c, Ksi $\sqrt{in.}$) at a 0.2% offset yield stress of 205,000 psi from centrally notched, fatigue cracked specimens using ink staining. (Data from Ref. 5.)
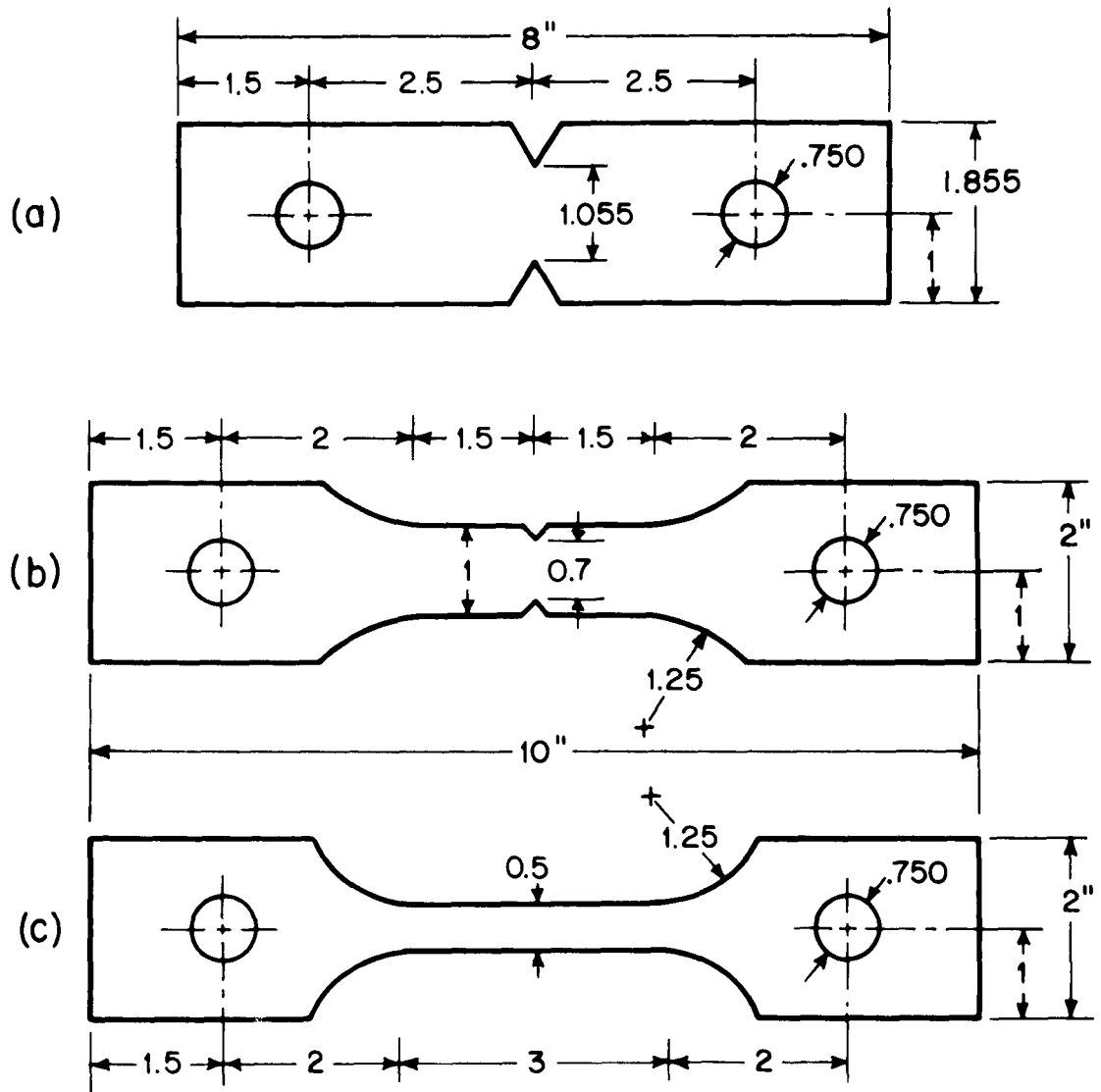
Figure I-1 - Test Specimens

3

II. EXPERIMENTAL PROCEDURE

1. **Specimen Preparation and Heat Treatment:** The AISI 4340 sheet from which all specimens were prepared, was air melted, sandwich cross-rolled and spheroidize-annealed. Its composition is given in Table I-2.

TABLE I-2

CHEMICAL COMPOSITION OF SHEET TESTED

	C	Mn	P	S	Ni	Cr	Mo	Si	Cu	V
Ladle	0.40	0.78	0.010	0.016	1.78	0.85	0.23	0.25	0.06	---
Sheet	0.40	0.80	0.007	0.017	1.79	0.83	0.22	0.23	0.05	0.025

All specimens were cut parallel to the long direction of a 0.108 in x 61 in. x 148 in. sheet. The three types of specimen prepared are described in Fig. I-1. The notch root radii of those of type (b) were 1.125, 0.125, 0.01 or less than 0.001-in., the last dimension being used with specimens for fracture-toughness determinations.

Specimens of type (a) were austenitized for one hour in argon at 1525°F and oil quenched. Specimens (b) and (c) were austenitized for twenty minutes at 1525°F in molten salt and then quenched into oil. All were refrigerated in liquid nitrogen within twenty minutes of quenching, air tempered for one hour, and oil quenched from the tempering temperature.

2. **Notch Sharpening:** The importance of obtaining notches sufficiently sharp to reduce the net fracture stress to the level associated with a "natural" crack has been widely emphasized.[7] Notch radii of less than .001 in. are currently specified. Since notching to radii less than about 0.002 in. by conventional machining is difficult and time consuming, notches were first milled in the edge-notched specimens and the root radius then reduced by a vibratory lapping operation designed for the purpose. Most consistent results were obtained by lapping the notch sharp prior to heat treatment, and then cleaning briefly again after heat treatment.

The apparatus for vibrolapping as finally evolved, is shown in Fig. I-2. The lapping compound is 1μ diamond paste while the lap is a single-edged razor blade driven with reciprocating movement by a vibrotool of the type used to mark metallographic specimens. As the blade is vibrated, a small weight(approximately 70 grams)holds it in the notch without stopping it, and a small-motor drive draws the blade slowly through the notch to distribute the blade wear more evenly. During one operation, a new blade is drawn back and forth squarely through the notch once a minute for five minutes, after which a new blade is inserted. Three such operations, with the side of the specimen facing the tool changed after each,
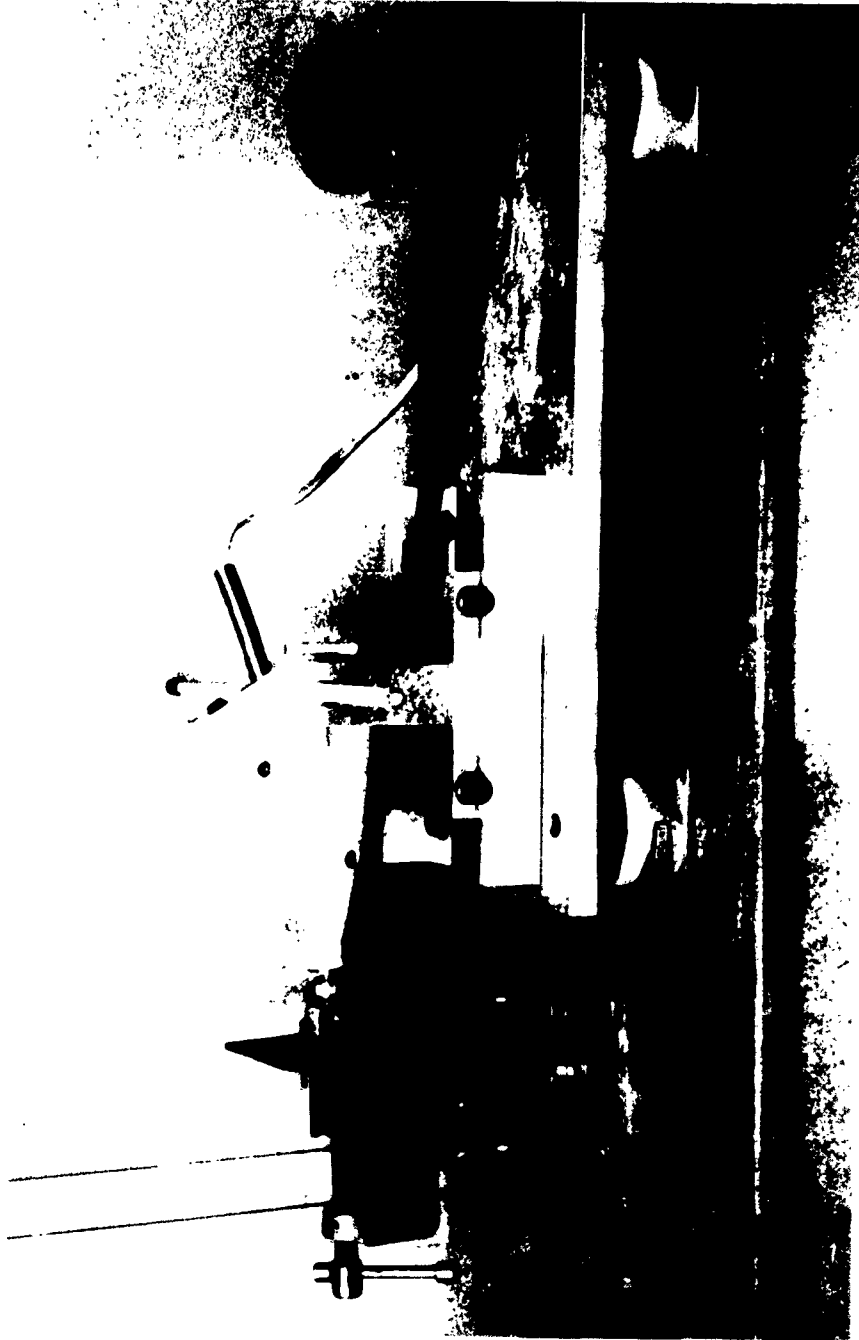
Figure I-2 - Equipment for Notch Sharpening by Vibrolapping. Pressure on Blade Applied by Weight (not shown) Hung on Neck of Vibrotool.

generally produced a satisfactory notch. A typical section through a sharpened notch is shown in Fig. I-3. Examination of the sharpened notches under the binocular microscope indicated that the notch was quite uniform along its length. The section shown in Fig. I-3 and the optical comparator examination of all specimens indicated that notch radii less than 0.00025-in. were produced by this technique.

3. <u>Observation and Estimation of Stable Crack Length:</u> Preliminary testing using ink staining to estimate the extent of slow crack growth indicated that the area of stable crack growth measured in this way corresponded closely to the triangular "porous tongue" on the fracture surface. Typical fractures are shown in Fig. I-4 in which these areas of slow growth are evident; sectioning of such cracks in an early stage, prior to fracture, (Fig. I-11) showed the porous appearance to result from numerous small cavities developing with the advancing crack. Accordingly, slow-crack growth was estimated from the extent of "porous tongue" on the fracture surface, not only because it was an easy and reliable technique but also because of the possibility that staining might induce stress-corrosion cracking, particularly in low fracture-toughness material. Of the two stable cracks (one at each notch root), that which did not accelerate to cause final fracture was assumed to give the length of the slowly growing crack at instability. The maximum length, h, of the roughly triangular porous area was measured and the crack length a calculated as

$$a = a_o + \frac{h}{2}$$

where a_o is the initial, machined notch length.

Stable cracks grew in discontinuous fashion. The clicking sound of the advance-arrest process could be detected during some tests by use of a stethoscope, which also made audible much slow crack growth not apparent to the ear alone.

4. <u>Measurement of Notch Symmetry:</u> The symmetry of the notch tips with respect to a line through the loading holes was determined in all fracture-toughness specimens. For measurement, a specimen was clamped on the table of a milling machine so that it could be translated exactly parallel or normal to the line through the loading holes. Grinding the specimen edges parallel to and equidistant from the center line through the holes, to within $\pm$ 0.0005 in., permitted the edges to be used for reference in lieu of the centerline. Linear distances, which were measured with a travelling microscope, were reproducible to within $\pm$ 0.0005 in.

The eccentricity of the notches was defined as $\Delta R = \sqrt{\Delta y^2 + \Delta x^2}$ with Δx and Δy as represented in Fig. I-5. Δx was measured directly; after measuring a_1 and a_2, Δy was calculated from

$$\Delta y = (\frac{W}{2} - a_1) - (\frac{W}{2} - a_2) = a_2 - a_1 \tag{1}$$
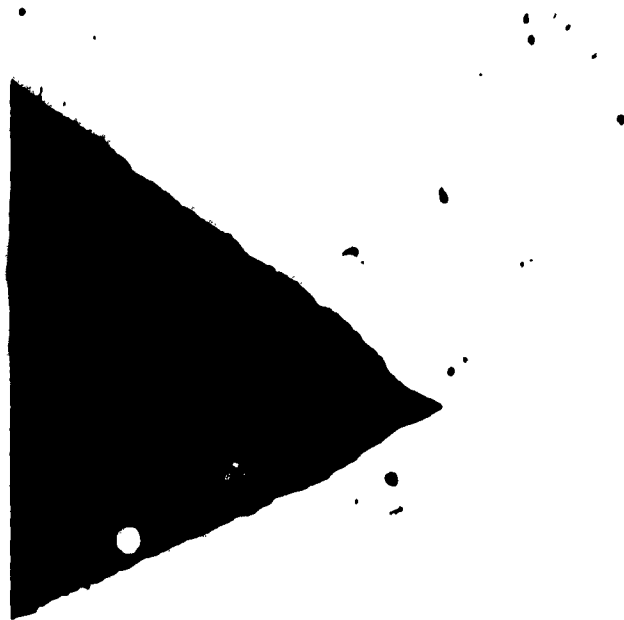
Figure I-3 - Section through a Typical Notch Produced by
Vibrolapping. Comparison Wire in Lower Left
has 0.001" Radius, 100X.

Fracture Surfaces of Sharply Notched AISI 4340 Stoel Sheet

Tempering Temperature   400°F

550°F

700°F

850°F
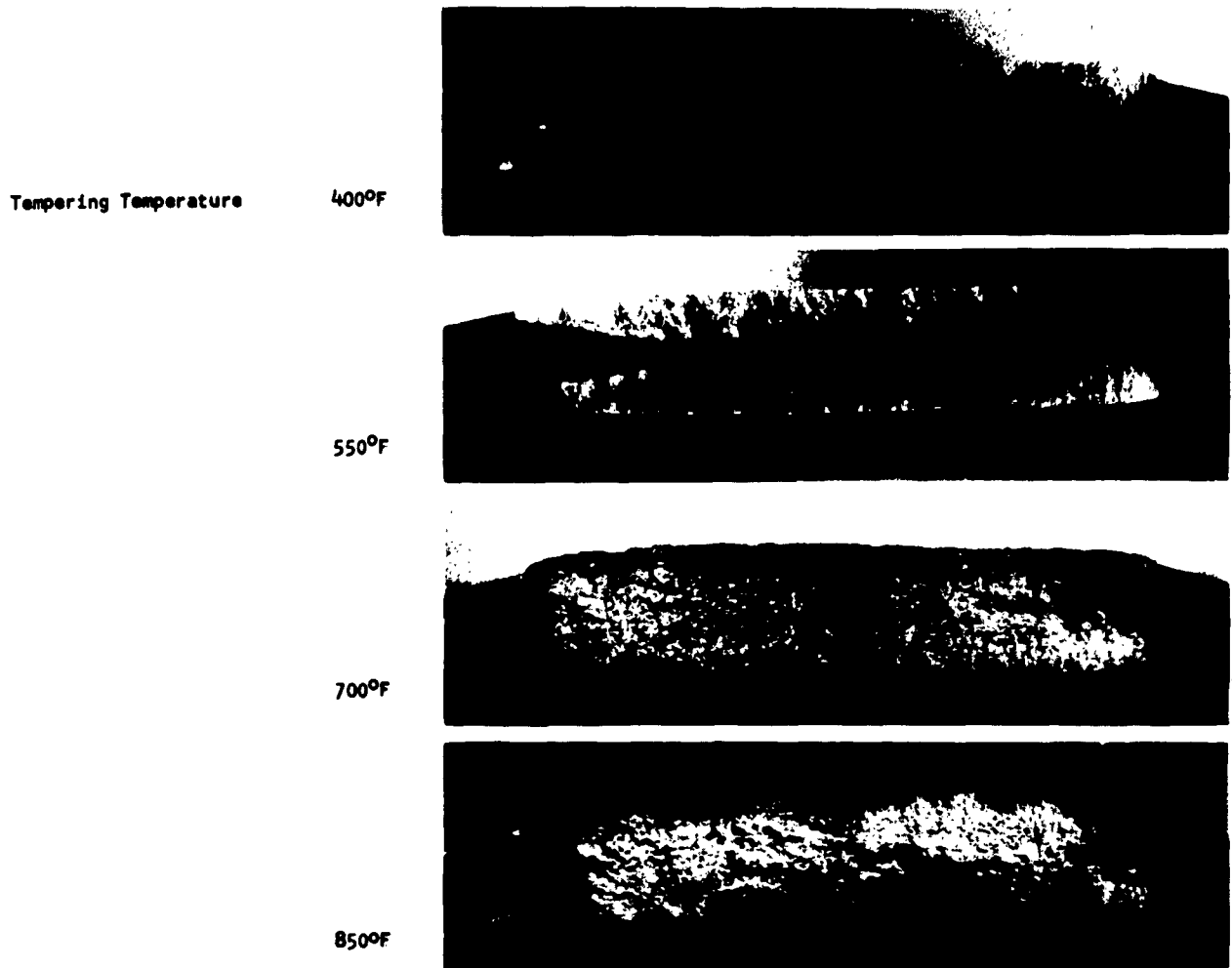
Figure I-4 - Typical Fractures of Sharply Notched Specimens
Illustrating Triangular Areas of Slow Crack
Growth. In Specimens Such as Those Tempered
at 400°F and 550°F the Rapid Crack Passed from
Left to Right and Hence the Size of the Slow
Crack on the Right is Measured.

8
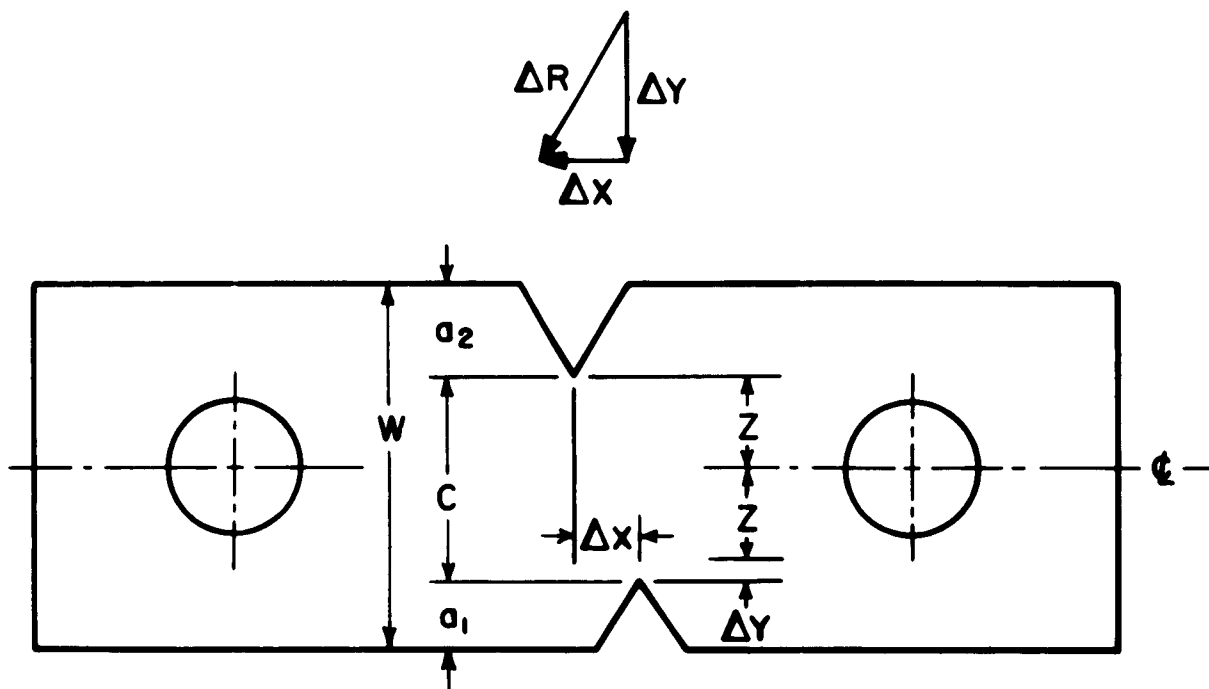
Figure I-5 - Dimensions Used in Defining Notch Symmetry.

The values obtained are given in Table I-3. If the ASTM specification[4] is interpreted as requiring that ΔR be less than 0.001W or, in the present case ΔR be less than 0.002 in., such a notch symmetry condition seems overly restrictive. For although $\overline{\Delta R}$ was 0.0037 in. including some values of ΔR as large as 0.008, it will be shown that the scatter in K_c is small suggesting that $\Delta R < .003W$ may be an acceptable symmetry specification.

5. **Fracture Examination:** After fracturing some specimens, one half was photographed and the other half nickel plated, sectioned and examined metallographically. The nickel was deposited at a current density of 0.1 to 0.15 amp. per sq. in. from a bath at $70^\circ F$ containing 300 gms of $NiCl_2 \cdot 6H_2O$ and 30 gms of H_3BO_3 crystals in a liter of water. Although the plate tended to peel on the flat areas, adherence was good on the fracture surface.

6. **Calculations:** Tensile data consisting of 0.2% offset yield strength, ultimate tensile strength and the strain-hardening exponent of the parabolic hardening equation were obtained from strip specimens of type (c) in Fig. I-1. Assuming strain hardening of the form $\sigma = A\epsilon^n$, n was obtained from the slope of the log σ - log ϵ relation by a least squares analysis. For this analysis the required true stress was calculated by dividing the load at any time by the area at the same time. The logarithmic (true) strain up to necking was calculated from the length changes in a 1 in. gage length obtained by visually aligning an adjustable length block with finely scribed reference marks.

Fracture toughness, K_c, for the edge-notched specimens (type (a)) was calculated in two ways. First, from the expression[4]

$$K_c = \sigma \sqrt{W \left[\tan \left(\frac{\pi a}{W} \right) + 0.1 \sin \frac{2\pi a}{W} \right]} \tag{2}$$

where

σ = gross section stress

W = gross section width

a = crack length at instability

The resulting K_c is considered "uncorrected" and applies to a finite-width sample of low fracture toughness in which plastic deformation at the notch tip is negligible. When plastic strains are significant, the following "corrected" expression is appropriate.[4]

$$K_c = \sigma \sqrt{W \left[\tan \left(\frac{\pi a}{W} + \frac{K_c}{2W\sigma_y^2} \right) + 0.1 \sin \left(\frac{2\pi a}{W} + \frac{K_c^2}{W\sigma_y^2} \right) \right]} \tag{3}$$

where σ_y is the tensile yield stress. A convenient graphical solution of Eq. 3 has been published.[4]

TABLE I-3

NOTCH SYMMETRY

Specimen	a_1	a_2	Δx	Δy	ΔR
D7	.3990	.4020	.0020	.0030	.0036
D10	.3980	.4045	.0027	.0065	.0071
D11	.3965	.3980	.0032	.0015	.0035
D12	.3970	.4010	.0000	.0040	.0040
D15	.3965	.3995	.0010	.0030	.0032
D16	.3955	.4015	.0007	.0060	.0060
D17	.3985	.4005	.0010	.0020	.0022
D18	.4030	.4040	.0020	.0010	.0022
D24	.3995	.4030	.0020	.0035	.0040
D27	.3960	.4040	.0005	.0080	.0080
E9	.4000	.4000	.0000	.0000	.0000
E12	.4020	.4030	.0043	.0010	.0044
E15	.3985	.4010	.0014	.0025	.0029
E20	.4045	.4035	.0033	.0010	.0034
E24	.3980	.4005	.0000	.0025	.0025
E25	.3990	.4015	.0000	.0045	.0045
E26	.3985	.4030	.0000	.0045	.0045
E27	.4010	.4015	.0012	.0005	.0013

$$\overline{\Delta x} = .0014 \qquad \overline{\Delta y} = .0028 \qquad \overline{\Delta R} = .0037$$

11

By analogy to an exact elastic-plastic solution for crack growth in torsion, McClintock[8] suggests that the radius of the plastic zone in a notched sheet specimen at instability is

$$R_c = B(\overline{RA}) \; \exp\left\{ \sqrt{2\left(\frac{e_\mu E}{\sigma_{TS}} - 1\right)} - 1 \right\} \tag{4}$$

where

e_μ = fractional elongation at necking of an unnotched strip specimen

σ_{TS} = tensile strength of an unnotched strip specimen

B = thickness of the specimen

$\overline{RA}$ = fractional reduction of area of a mildly notched specimen

Equation (4) applies when R_c is greater than B. The mildly notched specimen specified by McClintock is one 20B wide containing keyhole slots 5B deep at either edge with a root radius of B. In the present work, the reduction in area at fracture of type (b) specimens (Fig. I-1) with 0.125 in. radius notches was considered to approximate that of the required specimen. McClintock[8] further suggests that R_c is related to K_c by

$$K_c = \sigma_{TS} \sqrt{\pi R_c} \tag{5}$$

Thus, through Eq. (5) the fracture toughness of a material may be estimated from tensile data on an unnotched and a mildly notched sheet specimen.

III. RESULTS

The ultimate strength, yield strength, and hardness of unnotched strip specimens decreased with increasing tempering temperature (Fig. I-6) in a fashion consistent with the data of Shih, Averbach and Cohen[9] for round AISI 4340 specimens. The n values tended to decrease with increasing tempering temperature (Fig. I-7). The trend in the elongation at maximum load involved a minimum at tempering temperatures of 550°F and 700°F (Fig. I-7).

The effect of varying notch radius on the net fracture stress in sheet specimens of AISI 4340 is given in Fig. I-8. For radii of 0.125 in. or greater, the net stress at fracture is the same as that in the unnotched case. Upon tempering below 850°F, radii of 0.010 in. or less lead to fracture stress decreasing progressively with notch radius.

12
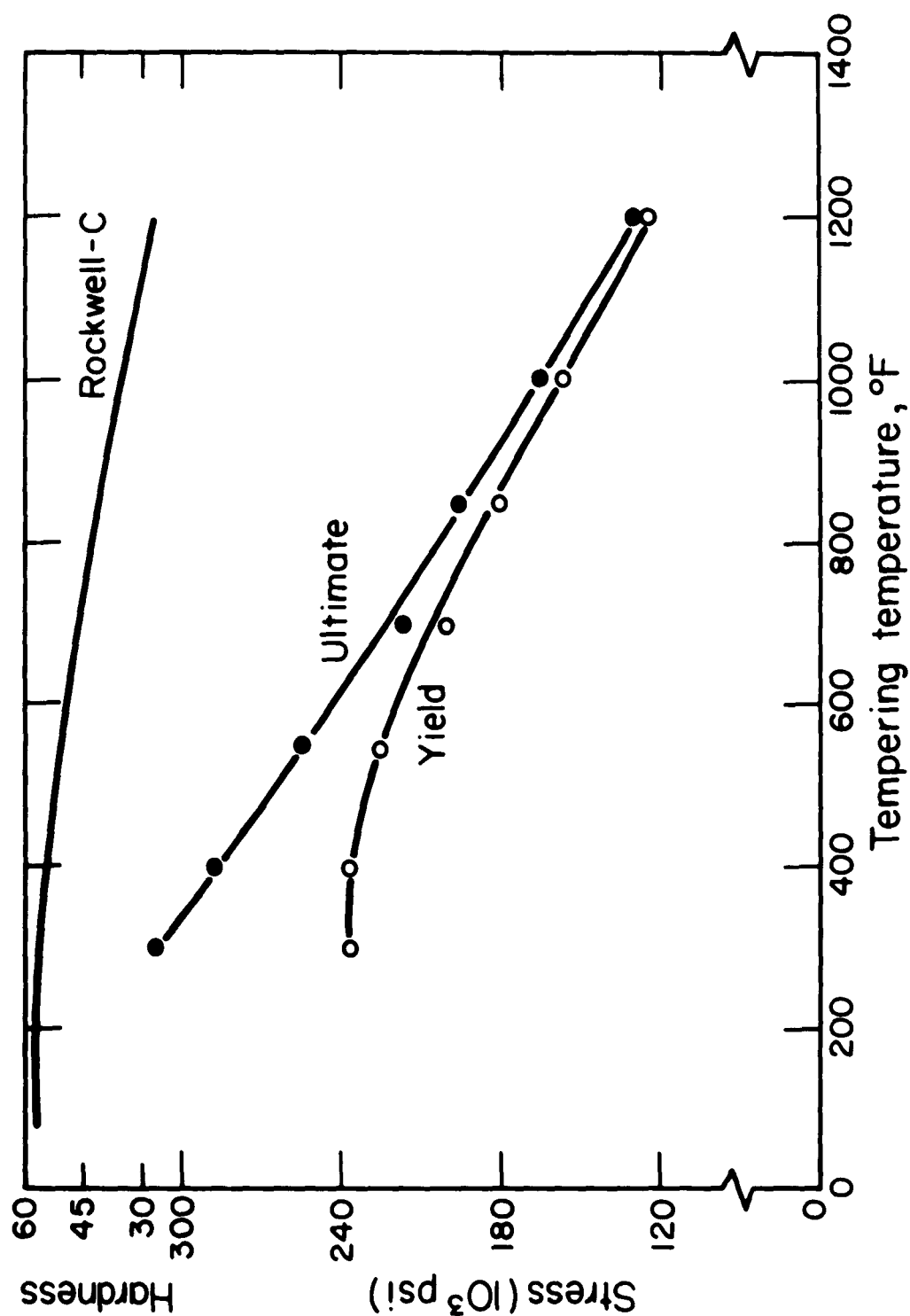
Figure I-6 - Effect of Tempering on Tensile Properties and Hardness of AISI 4340.

13
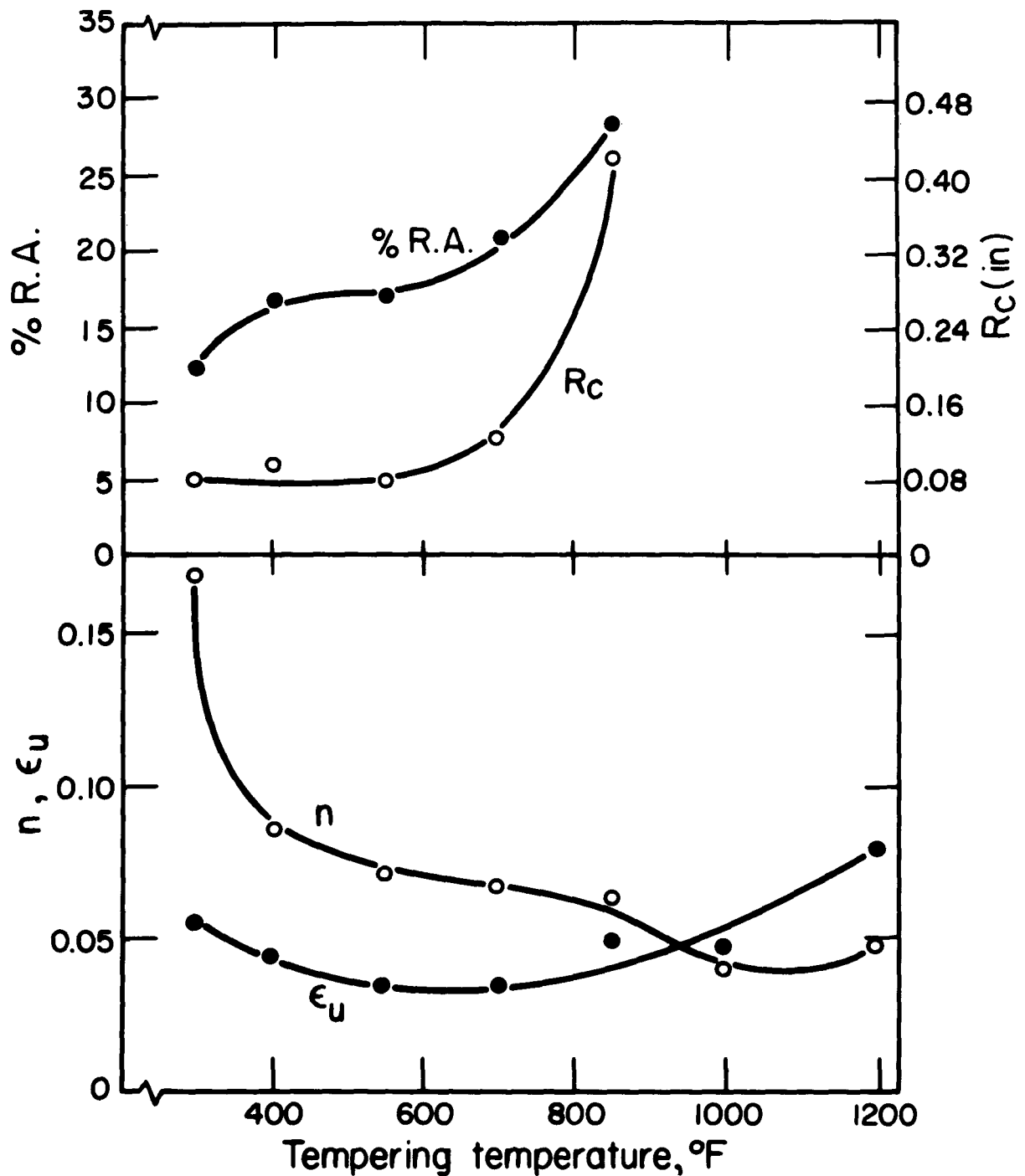
Figure I-7 - Effect of Tempering Temperature on Ductility and Strain
Hardening of AISI 4340 Steel.

R_c = plastic zone radius at instability from eq. (4)
%R.A. = area reduction at fracture in .125" root
         radius specimen
n   = strain hardening exponent of unnotched sheet
         specimen
e_u = fractional elongation at maximum load in an
         unnotched sheet specimen

14
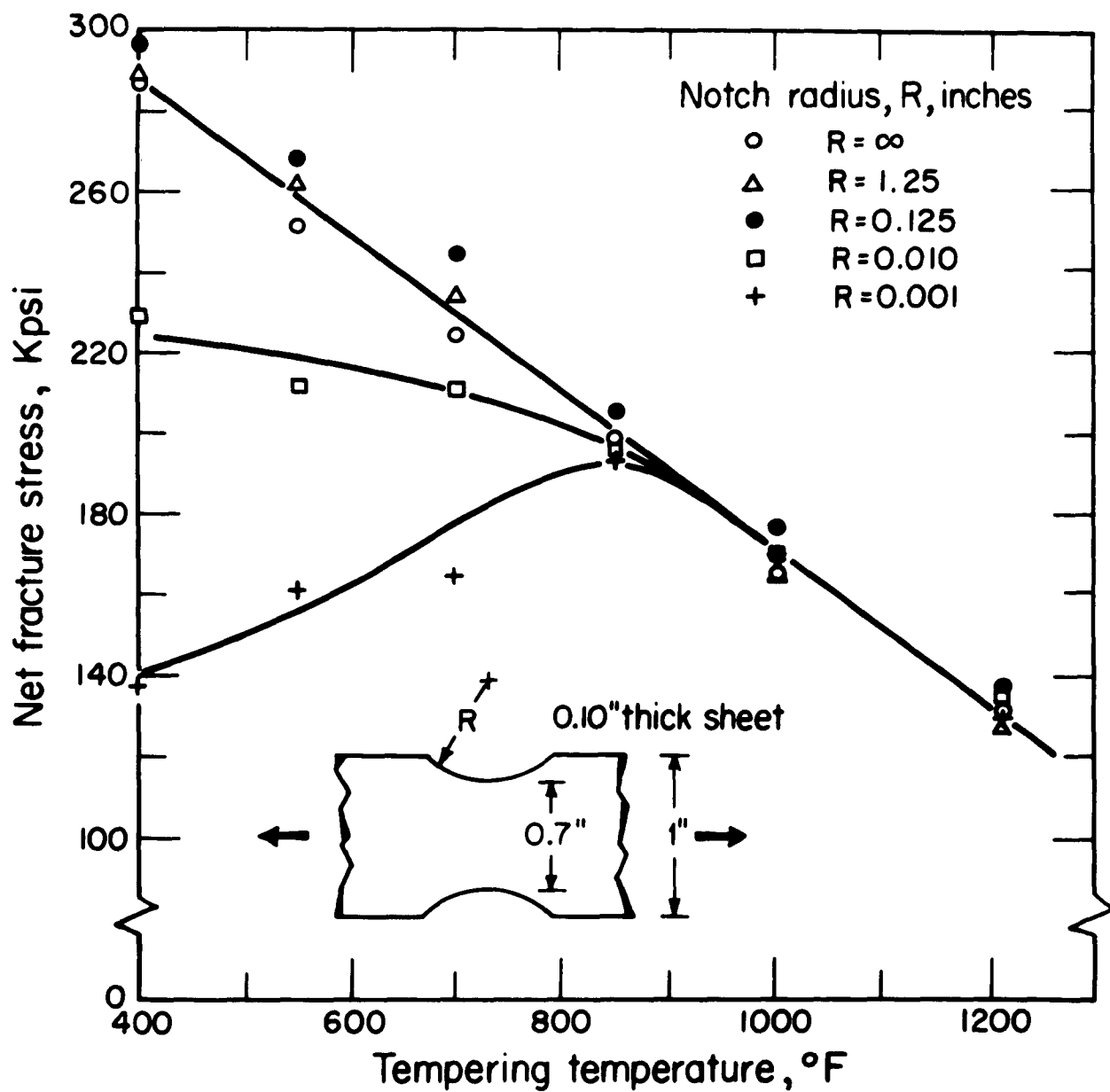
Figure I-8 - Effect of Tempering Temperature on Net Fracture Stress
of AISI 4340 Steel.

Fracture-toughness values calculated from data obtained with the sharpest notches are plotted in Figs. I-9 and I-10 as a function of tempering temperature for two width-to-thickness (W/B) ratios. The percentage of shear as commonly estimated from the fracture surface[4] is given in Fig. I-9. The width (W) only was varied in changing W/B. Even though the narrower specimens had a W/B ratio less than the 16 required by ASTM specification,[4] agreement in the calculated K_c values with the wider specimens was good. For specimens tempered over 400°F, the practical lower limit for AISI 4340, Eq. 3 gave increasingly higher values of K_c than Eq. 2.

In Fig. I-10 values of K_c according to the McClintock analysis are plotted on the basis of data from Fig. I-7. As shown in Fig. I-10, the analysis of McClintock and Irwin corrected for the effect of plastic zone agree closely for specimens tempered above about 550°F. McClintock restricts his analysis to cases where the plastic zone size, R_c, as calculated from Eq. (4) and plotted in Fig. I-7, is greater than B, a condition which is met for specimens tempered above about 600°F. The close correlation between the two analyses suggests that analytical methods for correcting K_c for plastic strain prior to crack instability are in relatively good order.

Stable (slow) cracks were formed in the testing of all specimens tempered at 400°F or above. In two instances (after tempering at 600°F and 1200°F) specimens suspected of containing such cracks, from the clicks emitted, were unloaded at 95 to 98% of the estimated fracture load, sectioned and microscopically examined. Sections were prepared by milling, either parallel or normal to the sheet surface, followed by metallographic polishing. Depending on tempering temperature, two types of crack patterns appeared. One, found in a specimen tempered at 600°F, consisted of a connected series of cavities as shown in Fig. I-11. The other, observed in a specimen tempered at 1200°F (Figs. I-12 to I-14), involved a network of cracks, which appears to be more nearly typical of highly tempered material and may be related to the fine "hair-line" cracks noted by Puttick[10] in ingot iron.

A common detail in the fracture surfaces was slipping or delamination parallel to the plane of the sheet. This occurred over both the flat-fracture areas, as shown in Fig. I-15, and on the macroscopic shear areas as well, Fig. I-16. In certain cases, inclusions were observed in the delaminations or in the paths of cracks extending from them (Fig. I-15c).

IV. DISCUSSION

The agreement between the Irwin analysis corrected for plastic zones and the equations suggested by McClintock is quite good over the range where R_c is greater than B (Fig. I-7). If the reduction in area of the mildly notched specimen could be inferred from the reduction in area of the unnotched strip specimen, the McClintock approach would provide a technique for deducing K_c for moderately notch-sensitive material from a simple strip tensile test. In its present state, however, McClintock's analysis must be regarded as tentative

16
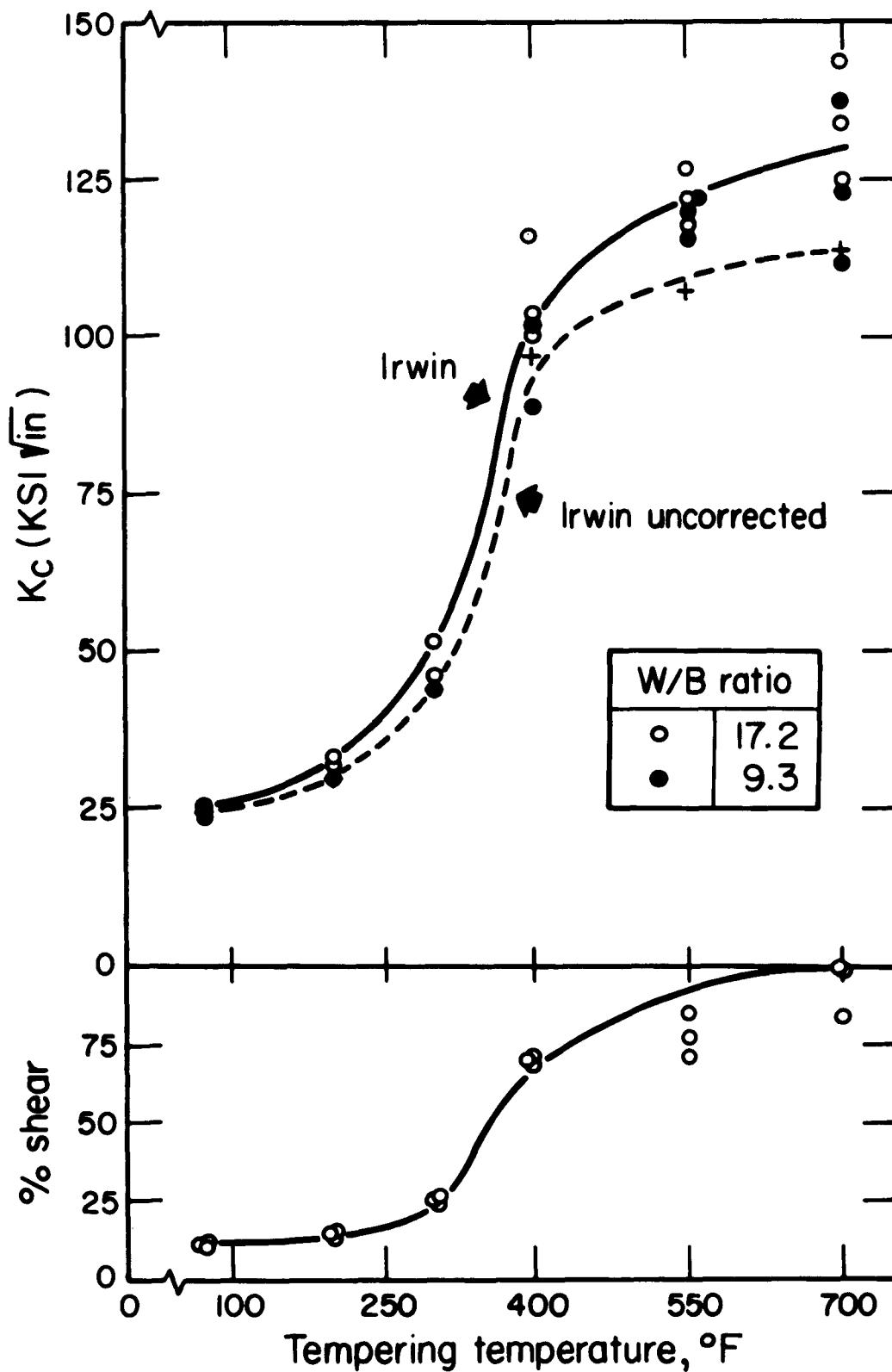
Figure I-9 – Effect of Tempering Temperature on Fracture Toughness and Percent Shear. Curve Marked "Irwin" is Based on Equation (3). Curve Marked "Irwin Uncorrected" is Based on Equation (2).

17
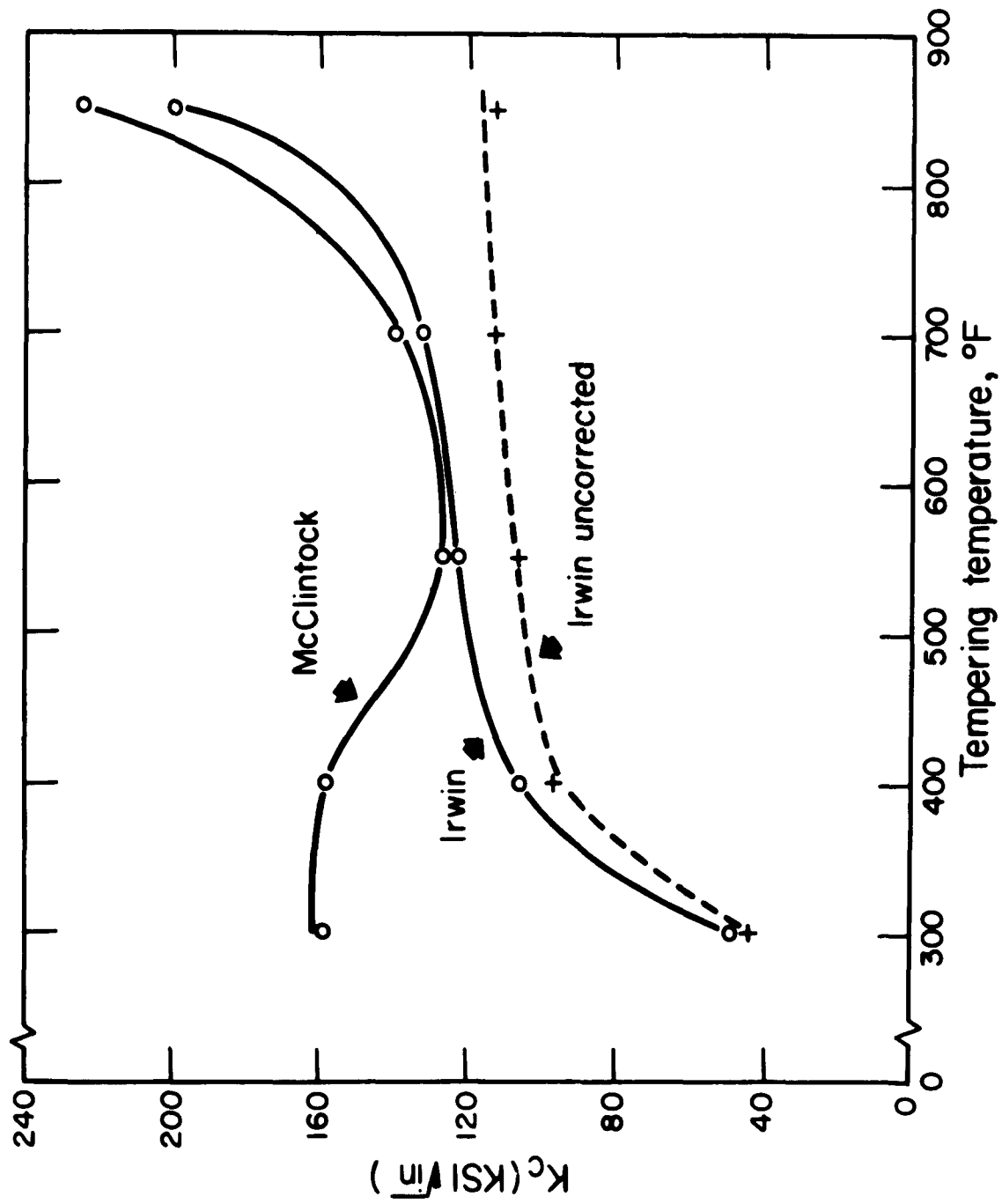
Figure I-10 - Effect of Tempering Temperature on Fracture Toughness as Determined by the McClintock and Irwin Methods.

18
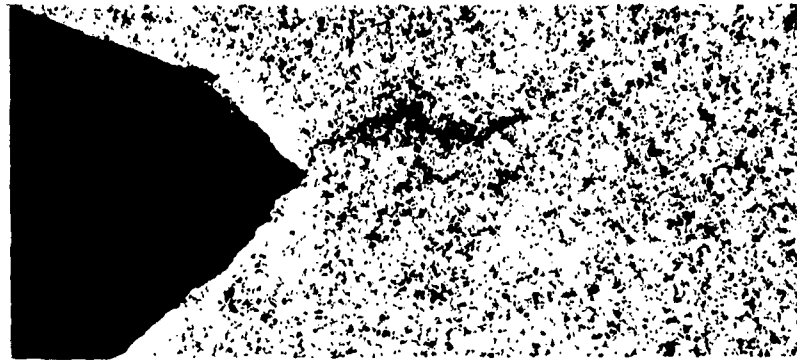
(a)

(b)
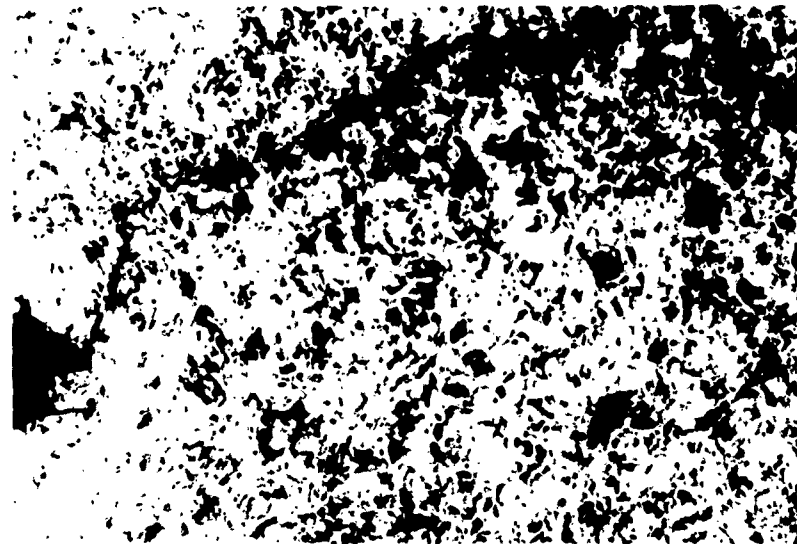
(c)

Figure I-11 - Specimen Tempered at 600°F Loaded to 98 Percent Estimated
Maximum Load, Showing Initiation of Stable Crack Growth
Beneath Notch Root: (a) 1 Percent Nital Etch, 75X,
(b) Unetched, 250X, (c) 1 Percent Nital Etch, 500X.

(a)

(b)

Figure I-12 - Stable Cracks at Notch Root in Specimen Tempered at
1200°F and Loaded to 95% of Estimated Maximum Load,
1 Percent Nital Etch: (a) Gross Tearing and Hair-
line Cracks, 100X, (b) Irregular Crack Growth,
1000X.

(a)

(b)

Figure I-13 - Same Specimen as in Fig. I-12 showing Onset of Oblique
Shear at Notch Root, Tempered at 1200°F: (a) Section
Through Stable Crack, Showing Shear Bands Growing from
Edge of Central Crack, unetched, approx. 30X, (b) Section
near the tip of the Stable Crack, Showing Pores Linking
up Along Oblique Shear Plane, unetched, approx. 35X.

(a)

(b)
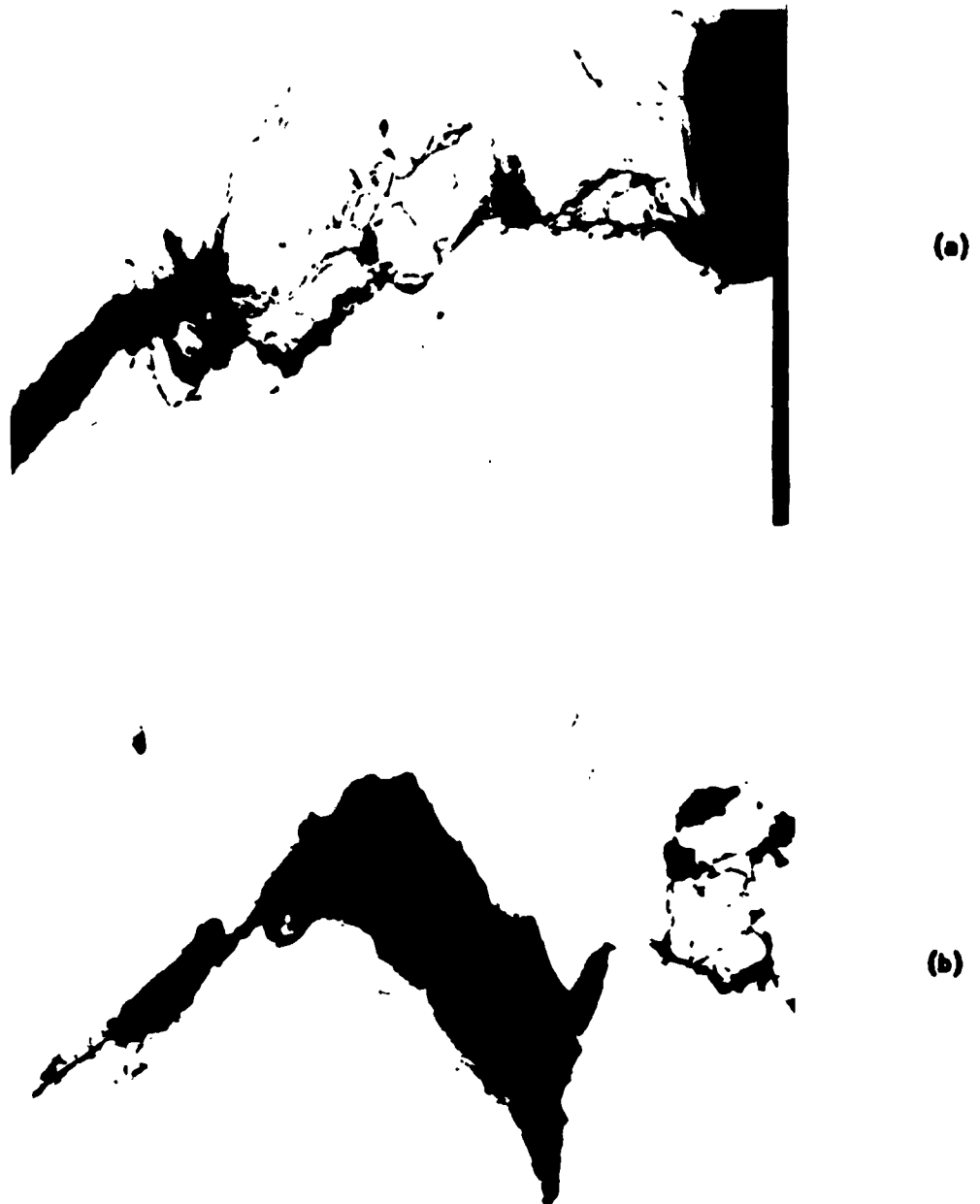
Figure I-14 - Same Specimen as Fig. I-12 Showing Void Formation Along
Oblique Shear Plane: (a) Heavily Strained Region Be-
tween Voids, 500X, (b) Agglomeration of Voids, Heavily
Strained Region at Void Edges, 500X.
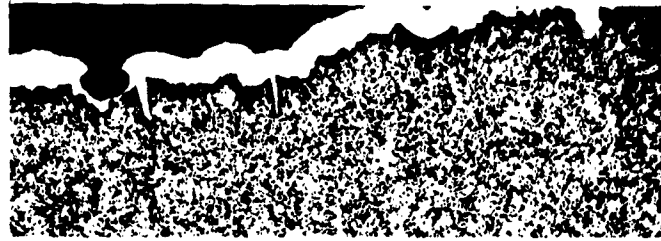
(a)

(b)
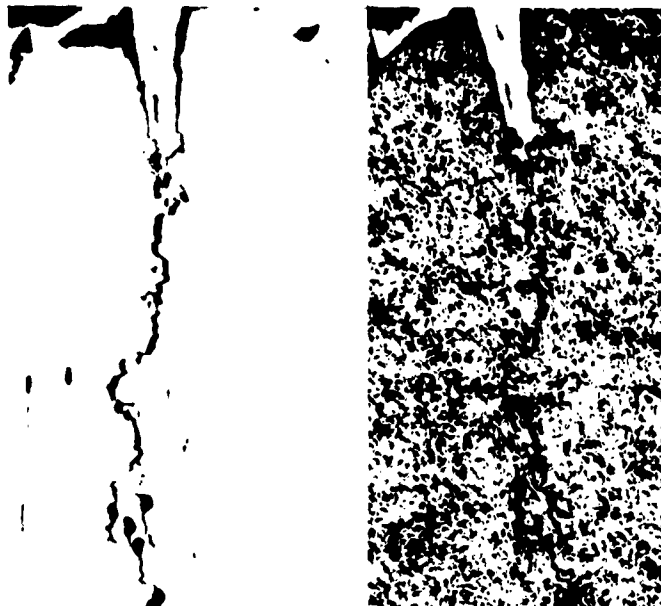
(c)

(d)

Figure I-15 - Fracture Surface of Specimen Tempered at 200°F, 1 Percent
Nital Etch: (a) Flat Fracture with Delaminations Along
Fibering Direction, 60X, (b) Jagged Secondary Cracks Along
Fibering Direction, 500X, (c) Unetched, Showing Jagged,
Discontinuous Crack Growth from Base of Delamination, 250X,
(d) Same as c, 250X.

(a)

(b)

Figure I-16 - Fracture Surface of Specimen Tempered at 700°F, 1 Percent
Nital Etch: (a) 100 Percent Oblique Shear, Approx. 40X,
(b) Delamination Along Fibering Direction, 500X.

since the method is based on a rather extended analogy involving terms with a physical relationship to fracturing that is difficult to establish.

(p.49)

In Fig. I-17, the fracture toughness data obtained in the present work is plotted together with Rawe's data on AISI 4340 prepared by air melting and unidirectionally rolling. The latter data relate to slightly thinner sheet than that of the present work (0.080 in. vs. 0.108 in.) and a longer total tempering time (2 + 2 hrs. vs. 1 hr.). Both variations should be reflected principally in vertical displacement of the K_c vs. tempering temperature curves, without affecting the scatter. As shown, the fracture toughness obtained for air-melted and cross-rolled material in the present work is intermediate between that for longitudinal and transverse specimens of air-melted material obtained in the other work. Such a result is reasonable and the basis for specifying cross rolling. The most striking feature of Fig. I-17, however, is the extent to which processing history influences the fracture toughness. Compared to the scatter in the individual determinations, which is typically no greater than about $\pm$ 20%, changing the processing history can introduce variations as great as 300%. The extreme sensitivity of K_c to processing history requires discretion in the use of tabulated K_c values in design and emphasizes the need for better understanding of how fracture toughness is affected by process variables.

The delamination observed so extensively raises the question of its having a possible role in the fracture process. In particular, it has appeared that one bridge between considerations of material structure and fracture toughness might be found in delamination, which is clearly a structural matter. Although the details of the delamination mechanism may not be fully established, it is recognized that the event is a consequence of a mechanical fibering and low fracture-resistance through the thickness of a sheet.

A potentially important reason for the suggestion relative to the delamination process is that fracture toughness, as measured by G_c or K_c, is frequently anisotropic. Accordingly, it would seem that elements of structure fixing the anisotropy must enter into the process determining the level of K_c, which means fibering in the broad sense but more specifically the mechanical fibering of elongated particles, secondary phases, etc. Also, the implication of this marked anisotropy is quite strong that the fracturing process does not involve crystallographic cleavage.

Furthermore, there are indications that fracture toughness takes on low values as thickness becomes very small, presumably due to localized, full-shear fracture with low energy absorption. Therefore, a possible sequence of events in the development of fast, unstable fracture might be:

1. Plastic deformation and transverse stresses at the crack tip acting to encourage delamination.

2. Fracture of the individual lamina in relatively small volumes (shear mode), resulting in low fracture toughness.

3. Over-all fast, relatively low-energy absorbing fracture, kept in a plane by the delaminating action.

Extending these speculations still further, the peculiar sharp temperature dependence of K_c could be introduced; it is rather striking that at temperatures where the generally recognized material properties are not strongly temperature dependent, K_c may increase by as much as a factor of 2 over a 100-200°F interval and fracture mode may go from little to full shear. The necessary additional suggestion is that the delamination tendency may be rather sharply temperature dependent.

Although the discussion relative to delamination is speculative, the outcome is a point of view with implications for fracture-toughness control. Specifically, higher fracture toughness ought to follow from suppressing delamination and improving the full-shear fracture toughness. Control of sheet-processing history should be a most effective way of regulating the delamination tendency.

V. SUMMARY

1. The measured fracture toughness, K_c, of air-melted and cross-rolled AISI 4340 sheet increased with tempering temperature, especially rapidly near 350 and 750°F. Comparison with the data of Rawe[5] indicates that for this steel the scatter in K_c due to variations in the processing history is much greater than the scatter due to variations in testing procedure.

2. A vibrolapping technique for sharpening of pre-machined notches in an edge-notched fracture-toughness specimen was developed which reduced the notch-root radius to less than 0.00025 in. This technique would seem to compete favorably with fatigue cracking of centrally notched specimens as a method for producing the sharp notches required in testing sheet material with fracture toughness less than about 100,000 psi $\sqrt{\text{in.}}$

3. Stable cracks were observed in all specimens tempered at 400°F (K_c = 100,000 psi $\sqrt{\text{in.}}$) or above. Single, stable cracks emanating from the notch tip were characteristic of specimens tempered at 600°F, whereas multiple, fine hair-line cracks, were characteristic of stable cracks in specimens tempered at 1200°F.

4. In all fractures examined, the material tended to split or delaminate in the rolling plane. Such a development may have a strong effect on the fracture toughness by reduction of the size of plastic zone accompanying the running crack. Further work on the relationship of the delamination tendency to processing history appears promising.

VI. REFERENCES

1. A.A. Griffith, Phil. Trans. of Royal Soc. (London) 221A (1920), p. 163.

2. E. Orowan, Fatigue and Fracture of Metals, John Wiley, New York (1952), p. 154.

3. G.R. Irwin, ASM Symposium, Fracturing of Metals, (1948), p. 152.

4. ASTM Bulletin, Jan. 1960, p. 29.

5. R. Rawe, Aerojet-General Corp., Report M2003, Feb. 1960.

6. S.Z. Uram, M.C. Flemings, and H.F. Taylor, Trans. AFS 68 (1960), p. 347.

7. Materials Research and Standards, Nov. (1961), p. 877.

8. F.A. McClintock, Discussion ASTM Bulletin, April (1961), p. 277.

9. C.H. Shih, B.L. Averbach and M. Cohen, Trans. ASM 48 (1956), p. 86.

10. K.E. Puttick, Phil. Mag. Ser. 8, 4 (1959), p. 964.

PART 2: EFFECT OF AUSTENITIZING TEMPERATURE ON
FRACTURE MODE OF AISI 4340

I. INTRODUCTION

The problems associated with the low ductility and fracture toughness of
hardened and tempered low-alloy steels are currently of much interest. These
steels, of which AISI 4340 is typical, are brittle in the as-quenched condition
and consequently are seldom used without tempering. With AISI 4340, for example,
a minimum practical tempering temperature is about 400°F. Shih, Averbach, and
Cohen[1] showed that the ductility of AISI 4340, as measured by the percent
reduction-in-area in tension, dropped abruptly for tempering temperatures below
400°F. In Part 1 it was demonstrated that the fracture toughness of this material
closely followed the ductility trend, also dropping abruptly when tempering was
done below 400°F.

One factor which may be involved in the brittleness of both as-quenched and
quenched and tempered steels is separation at prior austenite grain boundaries;
fracture along such a path would probably require little plastic work for its
propagation. Under at least three conditions of heat treatment, fracture in steel
may follow prior austenite grain boundaries: in overheated steel, in steel
tempered in the 500°F embrittlement range, and in as-quenched steel. The per-
sistence of facets, corresponding to prior austenite grain boundaries, in the
fractures of overheated steel is the basis of the definition and measurement of
the degree of overheating.[2] Grossman[3] and Baeyerts, Bumps and Sheehan[4]
have shown that the percentage of fracture along prior austenite grain boundaries
increases markedly for specimens tempered in the 500°F embrittlement range.
Lement, Averbach and Cohen[5] have suggested a precipitation leading to carbide
films at these sites. Turkalo's observation[6] that 50% of the fracture in an
as-quenched fine-grained steel (0.55% C, 1.30% Mn) broken in impact at 196°C
followed prior austenite grain boundaries suggests that cracking here may be a
contributing factor in as-quenched brittleness.

The interest in the present work was a correlation between fracture tough-
ness and fracture path. Since the amount of austenite grain boundary fracture
is difficult to estimate in fine-grained steel, some specimens with large prior
austenite grain size were examined. Thus, the study consisted of a comparison
of the fracture appearance of singly face-notched specimens austenitized at
1550 and 2300°F, oil quenched, refrigerated, tempered at various temperatures
and broken in impact bending at several temperatures. In addition, two con-
ventional edge-notched specimens were broken at room temperature after quench-
ing from 2300°F and refrigeration.

One shortcoming of any study such as this is the difficulty of relating
ductility or fracture toughness to fracture-topography examination of the
fracture. In the present work, a ductile (non-faceted) appearance was asso-
ciated with fracture toughness, the level increasing as topography became
rougher. It was realized that the surface roughness produced by passing the
crack through the thickness was probably greater than that produced by

a crack passing through the width. In addition to surface roughness and the amount of grain-boundary fracture, the relative amount of delamination, the tendency for splitting to occur along the rolling plane at its intersection with the fracture surface, was noted.

II. EXPERIMENTAL PROCEDURE

The same sheet of air melted and cross-rolled AISI 4340 steel described in Part I was used here. Specimen dimensions are given in Fig. II-1. All were cut from the sheet with their long axis parallel to the long axis of the specimens in Part I, so that the plane of fracture had the same orientation in the sheet in both cases.

The specimens were wired together and austenitized within a zircon tube heated in a silicon-carbide resistance furnace. After one hour at temperature the vacuum was broken and followed by quenching in oil. It was estimated by later metallographic examination that 0.0005-0.001-in. of scale formed during the approximately 30-second period that hot specimens were in air. Immediately after quenching the specimens were refrigerated in liquid nitrogen and stored at that temperature until tempered for one hour in a circulating air furnace.

Two austenitizing temperatures were used, 1550 or 2300°F. The former led to a grain size of ASTM 7-8, while the latter gave a grain-size number less than 1, according to the ASTM comparative method; the mean grain diameter in the latter case was about 0.025 in.

The specimens were broken by clamping one half in a vise and striking the protruding half with a hammer. For testing at other than room temperature, a specimen, mounted in the vise, was placed first in a constant temperature bath. After reaching bath temperature it was removed and broken within 3 seconds. The testing temperatures were -346°F (boiling liquid nitrogen), -109°F (acetone and dry ice), 70°F (room temperature), 212°F (boiling water).

Immediately after fracture the surface of one half was nickel plated by the technique described in Part I. Then an arbitrary section through the fracture surface normal to the notch was made with an abrasive wheel and the section freed by a cross cut. The freed piece was mounted, polished, etched and photographed. The etchants used are shown in Table II-1. Etch No. 2 revealed prior austenite grain boundaries in specimens austenitized at 2300°F but not at 1550°F. Etch No. 1 was used to bring out the martensite structure after quenching from the lower temperature. The other half of the broken specimen was placed in a plastic envelope containing a vapor-phase rust inhibitor for subsequent observation and hardness determination.
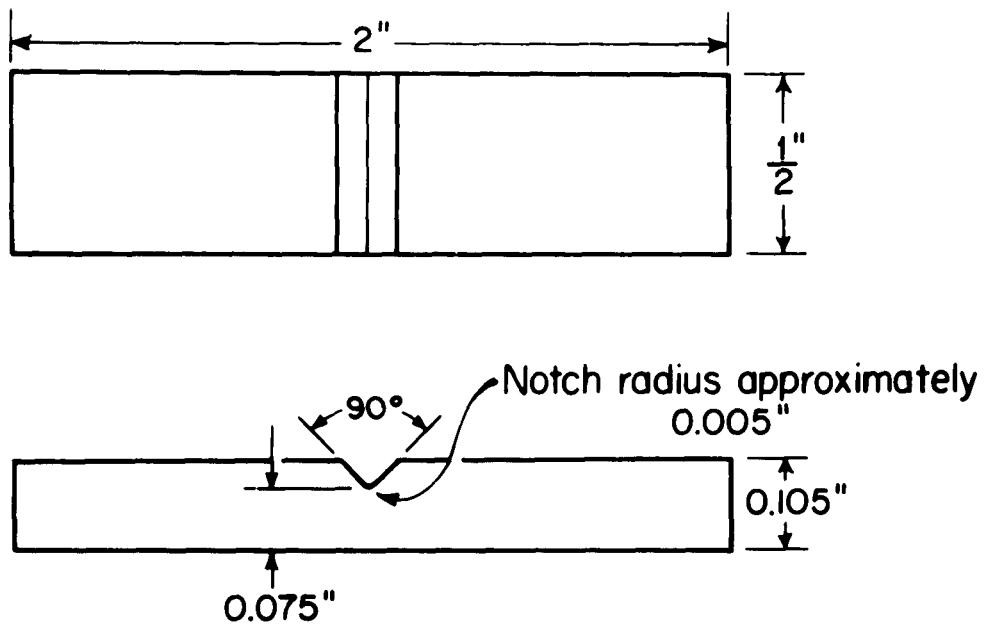
Figure II-I - Face Notched Test Specimen

TABLE II-1

ETCHANTS EMPLOYED IN METALLOGRAPHY

Austenitizing Temperature	Etchant
1550°F	(1) 1% nital
2300°F	(2) 1 gram picric acid 1 ml HCl (36%) 100 ml. methyl alcohol

Two edge-notched specimens, 1-in. wide with 0.20-in. deep notches, were prepared to measure the fracture toughness of coarse-grained, as-quenched material. After machining and preliminary notch sharpening by vibrolapping, they were covered with a thin refractory coating, austenitized for one hour at 2300°F in mechanical vacuum, oil quenched, and placed in liquid nitrogen. The notches were again cleaned and sharpened by a short period of vibrolapping. Surface grinding, with a large excess of coolant, symmetrically reduced the thickness to .063 in., giving W/B = 16 and removed any surface pits. The average hardness was 56 Rockwell-C on ground surface and 55 on the adjacent unground surface, indicating that any decarburization was slight.

Slow crack propagation in one of the edge-notched samples was measured by staining with recorder ink; in the other the total was estimated from the fracture surface. In both cases the progress of the stable crack could be followed with a stethescope.

III. RESULTS

The Rockwell-C hardness of the face-notched specimens austenitized at 1550°F and 2300°F, and specimens austenitized at 1525°F from Part I are plotted in Fig. II-2 as a function of tempering temperature. The lower hardness of those austenitized at 2300°F and tempered below 400°F is probably due to decarburization. It was later found that the refractory coating led to higher as-quenched hardness (about 55 R_C), indicative of less carbon loss during austenitizing. The surfaces of the as-quenched and broken refractory-coated specimens contained about 20% intercrystalline fracture, in contrast to about 10% for those heat treated without coating. Thus fracture mode is somewhat sensitive to carbon level in this carbon range. The amount of intercrystalline fracture in as-quenched coarse-grained samples was not altered by eliminating the liquid-nitrogen quench or introducing the notch after heat treatment.

31
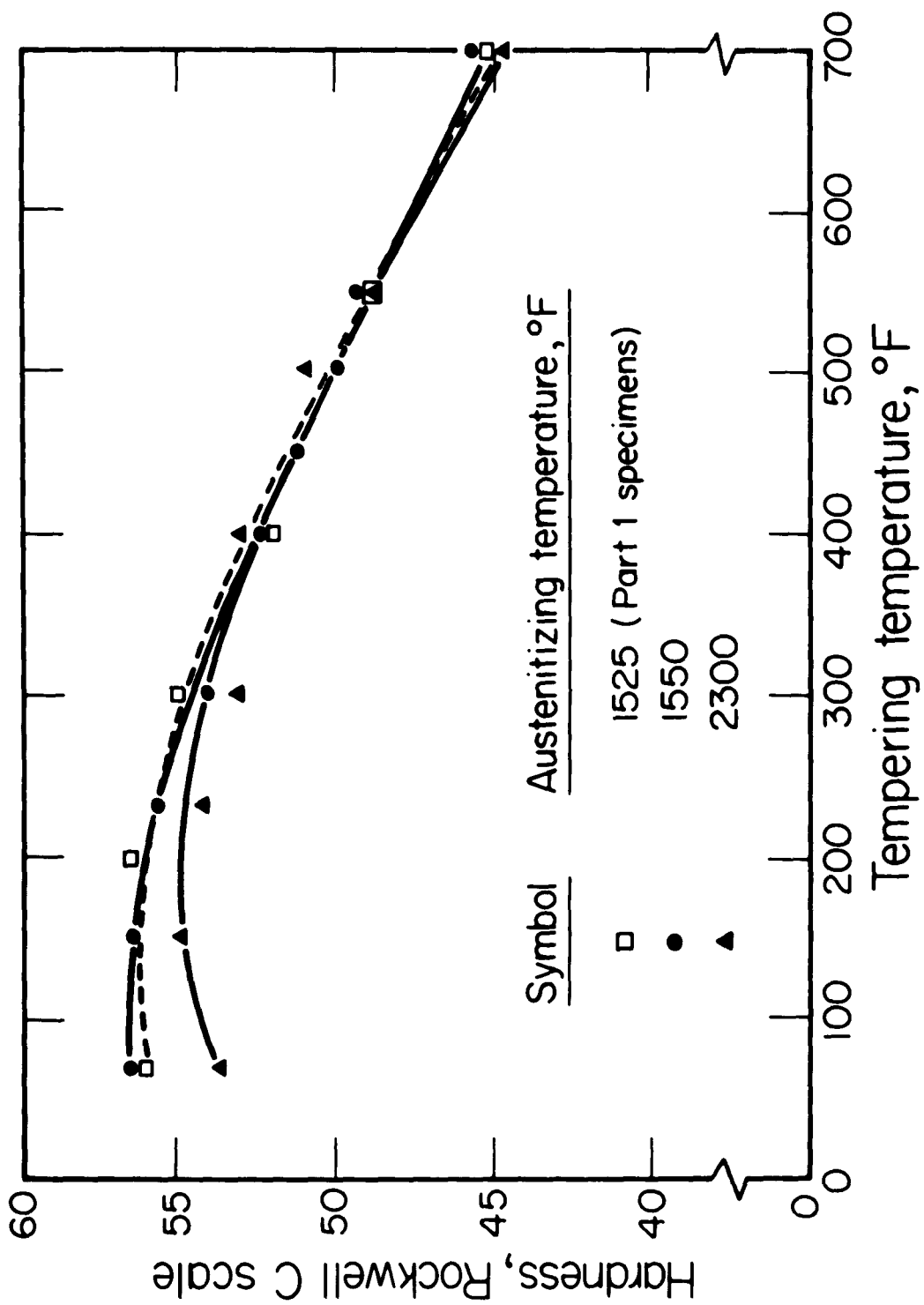
Figure II-2 - Hardness of Test Specimens after Tempering for One Hour.

As Quenched Observations: As-quenched fracture surfaces appear tougher for the material of larger austenite grain size, as comparison of Figs. II-3 and II-4 shows. In support of this qualitative indication, K_c values for the as-quenched coarse-grained specimens measured with edge-notched strips are given in Table II-2 along with the values for as-quenched fine-grained specimens from Part I. Since K_c for specimen B12 is probably low owing to corrosion by the staining ink, data on unstained specimen B21 indicates an increase in K_c of 3-4 times with the higher austenitizing temperature. The stress relief effected by refrigeration in liquid nitrogen, the delamination tendency of the steel, the relative thinness of the specimen and the loading rate may all influence the observed toughness of untempered martensite formed from coarse-grained austenite. In this tougher, as-quenched condition, slow intergranular cracking was a prominent feature of the fracture. As heard in the stethescope, slow crack-growth started at about 60% of the fracture load and continued to fracture. There were two distinct parts to the fracture, a portion identified with the slow intergranular cracking, which was quite extensive, and the remainder of essentially 100% shear associated with rapid fracturing. Ink staining established that the intergranular cracking occurred slowly. Interestingly, the ink also increased the rate of crack extension at constant load; the cracking to be heard with the stethescope increased markedly when more ink was added to the notch, even at constant load greater than that to start the slow crack. Such a stress-corrosion effect undoubtedly accounts for the lower K_c of the stained specimen.

Tempering: Effects of tempering after the different austenitizing treatments are brought out in Figs. II-3 to II-11. In considering only the 1550°F austenitizing treatment, surface roughness is small for tempering at 70 and 150°F (Figs. II-3 and II-4 top), increases rapidly with tempering between 300 and 500°F (Figs. II-6 through II-9 top) and then increases slowly with further increases in tempering temperature (Figs. II-10 and II-11 top); qualitatively, one might anticipate a parallel trend in fracture toughness, as was in fact demonstrated in Fig. I-9.

In the case of 2300°F austentiizing, surface roughness is slightly greater after tempering at 400-450°F (Figs. II-7 and II-8 bottom) than in the as-quenched condition. The amount of grain boundary fracture upon tempering at 150°F and 230°F is somewhat greater, in comparison to the as-quenched and 400°F observations. Thus one might infer that the fracture toughness of coarse-grained material decreases a little as tempering temperature is raised to about 200°F and then increases with further increase in tempering temperature to the range 400-450°F.

All comparisons (Figs. II-5 to II-8) show greater surface roughness in the coarse-grained fractures for tempering temperatures to 450°F. Thus a further implication is greater fracture toughness for the coarse-grained material tempered between 70-450°F.

Fracture after austenitizing at 2300°F and tempering at 550°F and 700°F follows prior austenite grain boundaries almost exclusively (Figs. II-10 and II-11 bottom) as indicated in Fig. II-17. The observation agrees with that of Baeyertz, Bumps and Sheehan and Grossman, whose data are included in Fig. II-17. All such observations establish the intercrystalline nature of fracture in coarse, and probably fine, grained specimens tempered in the 500°F "embrittlement range".

33

Figure II-3 - Top: Sample H, Austenitized at 1550°F, Tempered at
                       70°F, Broken at 70°F

          Bottom: Sample MM, Austenitized at 2300°F, Tempered at
                    70°F, Broken at 70°F

          Magnifications: Sections, 50X; Fracture Surfaces, 7X
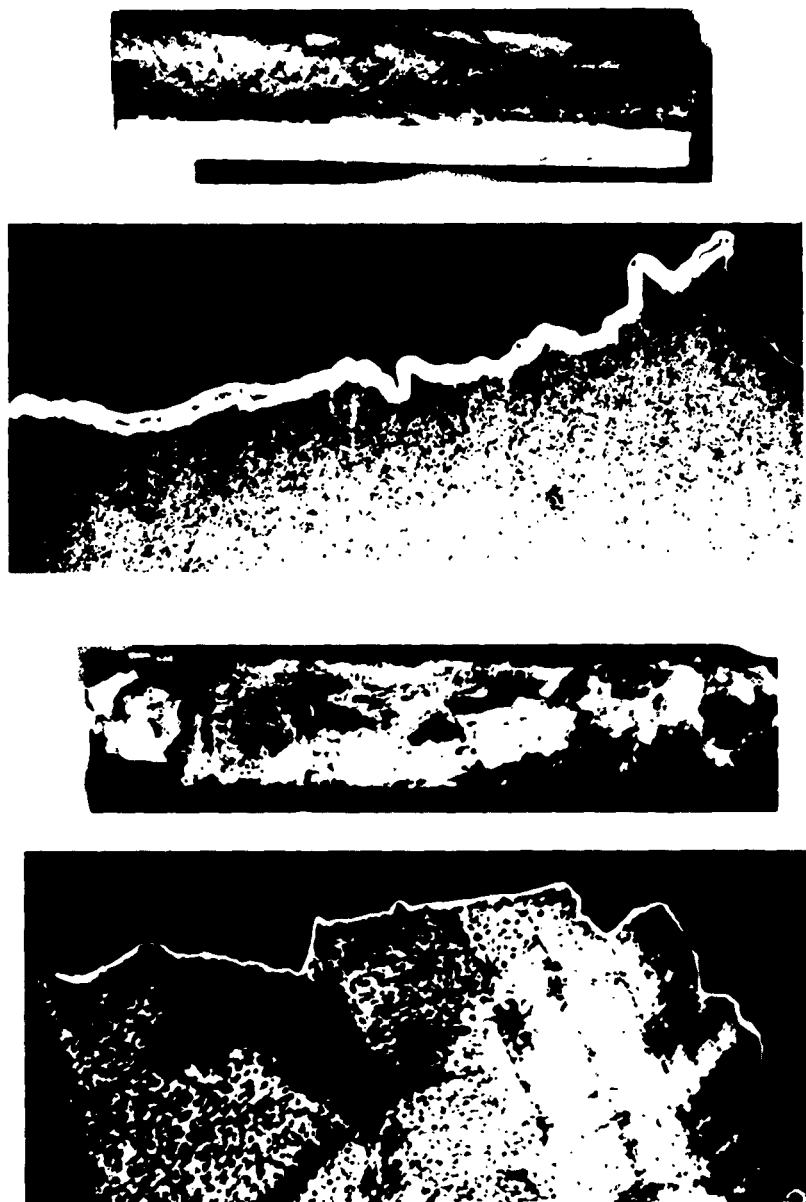
Figure II-4 - Top: Sample B, Austenitized at 1550°F, Tempered at 150°F, Broken at 70°F

Bottom: Sample LL, Austenitized at 2300°F, Tempered at 150°F, Broken at 70°F

Magnifications: Sections, 50X; Fracture Surfaces, 7X

35

Figure II-5 - Top: Sample E, Austenitized at 1550°F, Tempered at 230°F, Broken at 70°F

            Bottom: Sample JJ, Austenitized at 2300°F, Tempered at 230°F, Broken at 70°F

            Magnifications: Sections, 50X; Fracture Surfaces, 7X
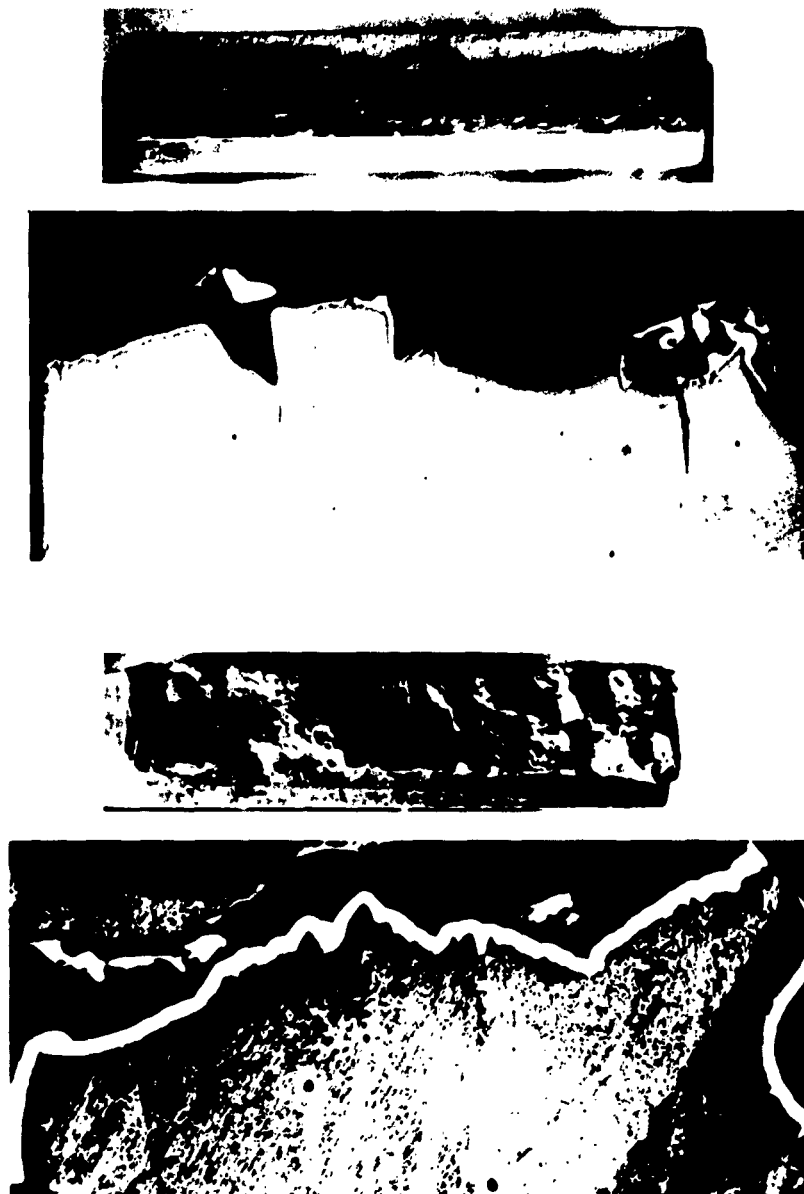
Figure II-6 - Top: Sample L, Austenitized at 1550°F, Tempered at
                      300°F, Broken at 70°F. This Specimen was
                      Etched with 4% Picral.

          Bottom: Sample CCC, Austenitized at 2300°F, Tempered
                    at 300°F, Broken at 70°F

          Magnifications: Sections, 50X; Fracture Surfaces, 7X
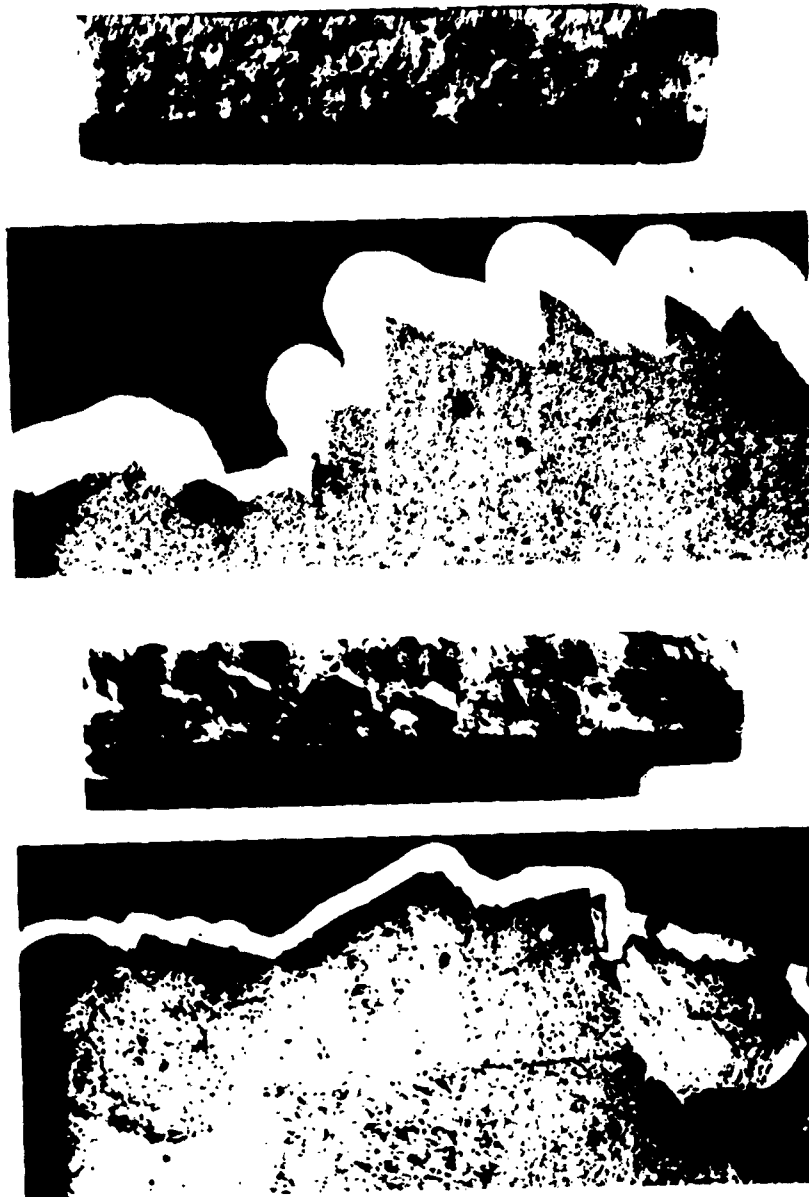
Figure II-7 - Top: Sample K, Austenitized at 1550°F, Tempered at
                      400°F, Broken at 70°F

          Bottom: Sample FF, Austenitized at 2300°F, Tempered at
                   400°F, Broken at 70°F

          Magnifications: Sections, 50X; Fracture Surfaces, 7X
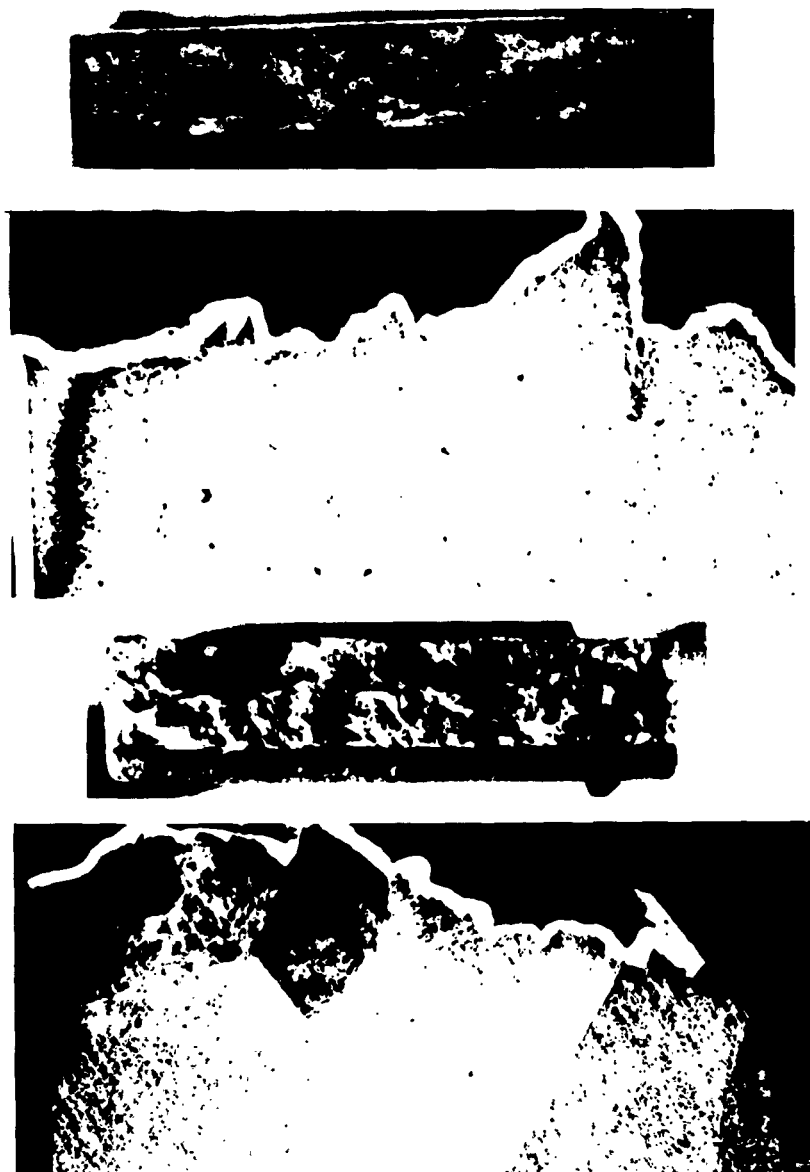
Figure II-8 - Top: Sample G, Austenitized at 1550°F, Tempered at
                       450°F, Broken at 70°F

           Bottom: Sample BB, Austenitized at 2300°F, Tempered at
                       450°F, Broken at 70°F

           Magnifications: Sections, 50X; Fracture Surfaces, 7X
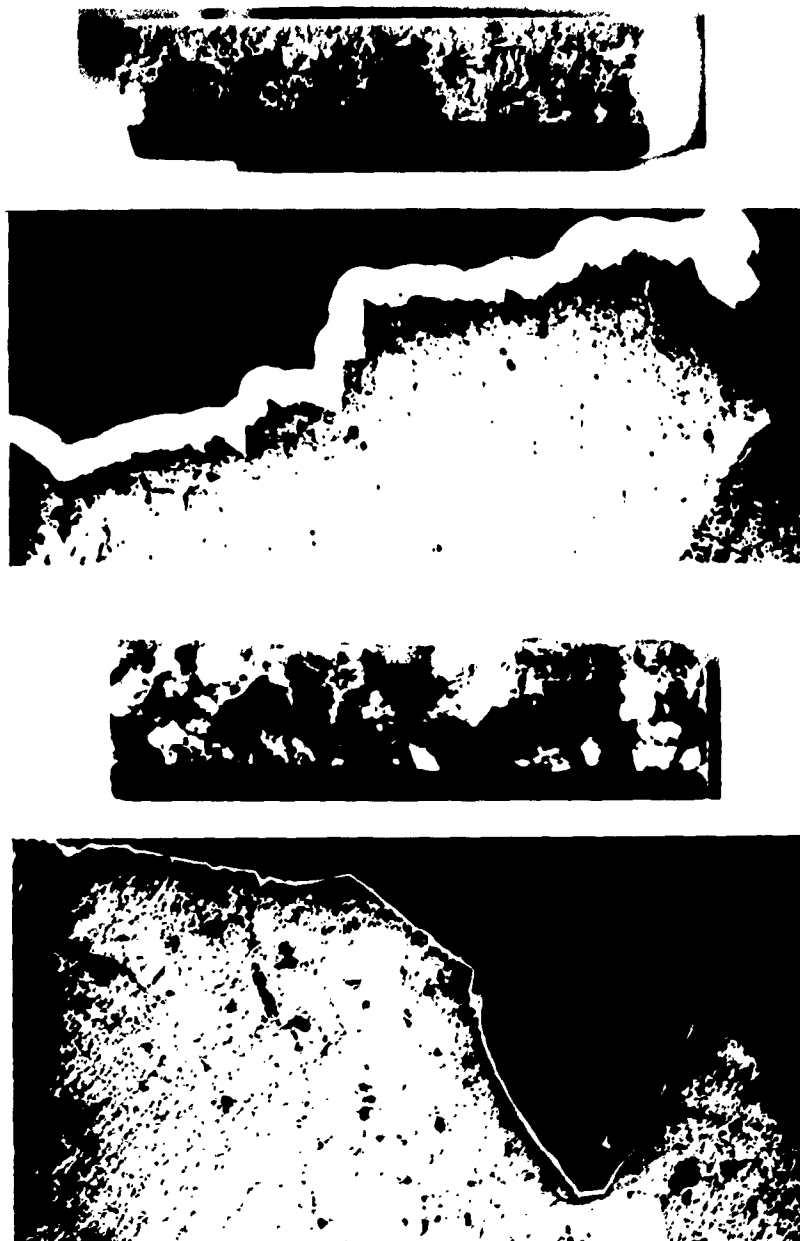
Figure II-9 - Top: Sample C, Austenitized at 1550°F, Tempered at
                      500°F, Broken at 70°F

          Bottom: Sample HH, Austenitized at 2300°F, Tempered at
                    500°F, Broken at 70°F

          Magnifications: Sections, 50X; Fracture Surfaces, 7X

40
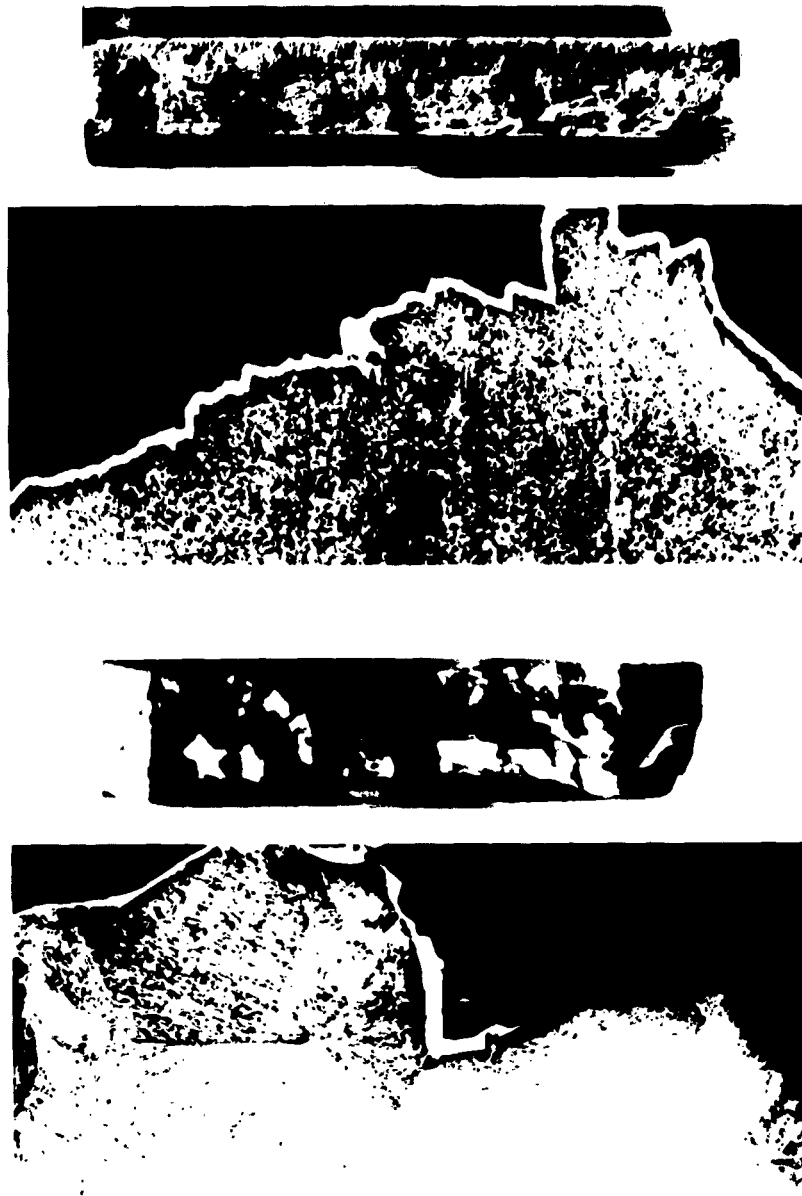
Figure II-10 - Top: Sample D, Austenitized at 1550°F, Tempered at
                         550°F, Broken at 70°F

          Bottom: Sample DD, Austenitized at 2300°F, Tempered at
                   550°F, Broken at 70°F

          Magnifications: Sections, 50X; Fracture Surfaces, 7X
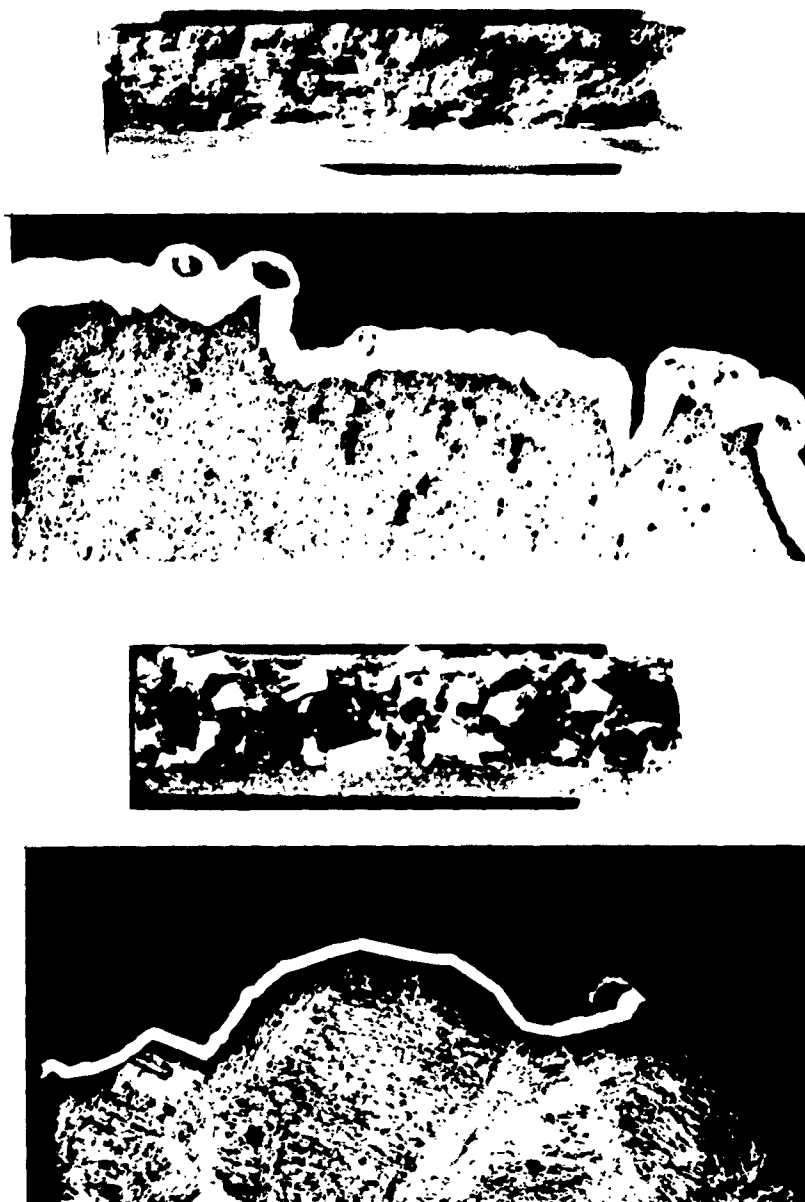
Figure II-11 - Top: Sample M, Austenitized at 1550°F, Tempered at
                        700°F, Broken at 70°F

          Bottom: Sample EE, Austenitized at 2300°F, Tempered at
                   700°F, Broken at 70°F

          Magnifications: Sections, 50X; Fracture Surfaces, 7X

TABLE II-2

FRACTURE TOUGHNESS OF AS-QUENCHED EDGE-NOTCHED SHEET SPECIMENS

Specimen	Hardness, R_c	Austenitizing Temperature °F	K_c psi $\sqrt{in.}$	Remarks
E 15	56	1525	26,000	----
E 20	55.5	1525	26,600	----
E 24	56	1525	26,000	----
B 12	55	2300	85,000	stained
B 21	55	2300	90,000	unstained, slow crack taken as intergranular portion of fracture
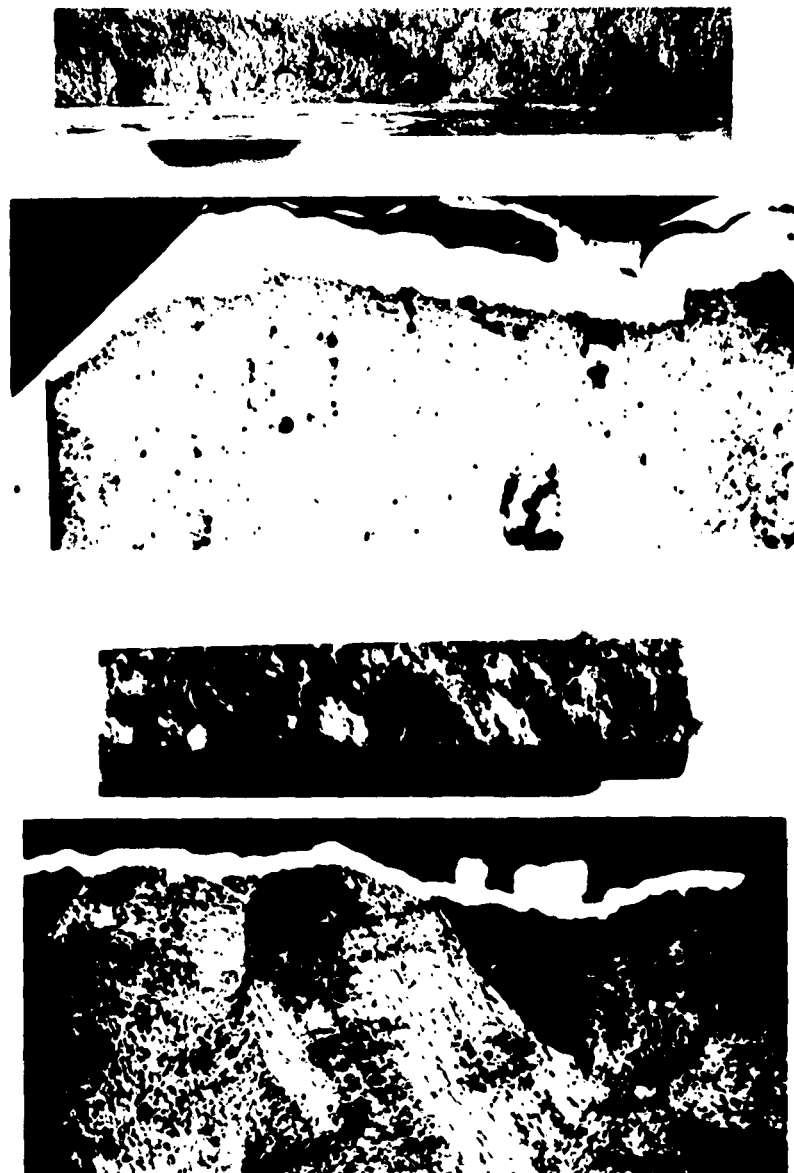
Figure II-12 - Top: Sample AAA, Austenitized at 1550°F, Tempered at
                        400°F, Broken at -346°F

          Bottom: Sample U, Austenitized at 2300°F, Tempered at
                        400°F, Broken at -346°F

          Magnifications: Sections, 50X; Fracture Surfaces, 7X
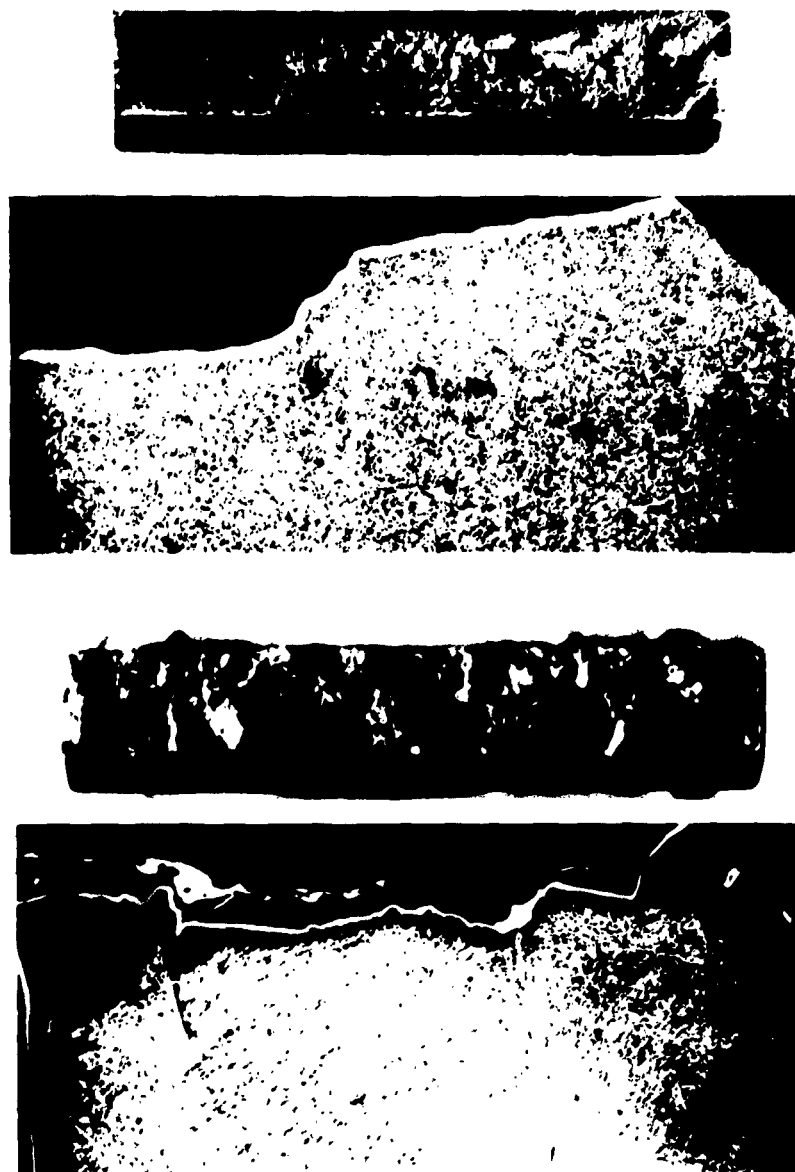
Figure II-13 - Top: Sample A, Austenitized at 1550°F, Tempered at 400°F, Broken at -109°F

            Bottom: Sample X, Austenitized at 2300°F, Tempered at 400°F, Broken at -109°F

            Magnifications: Sections, 50X; Fracture Surfaces, 7X
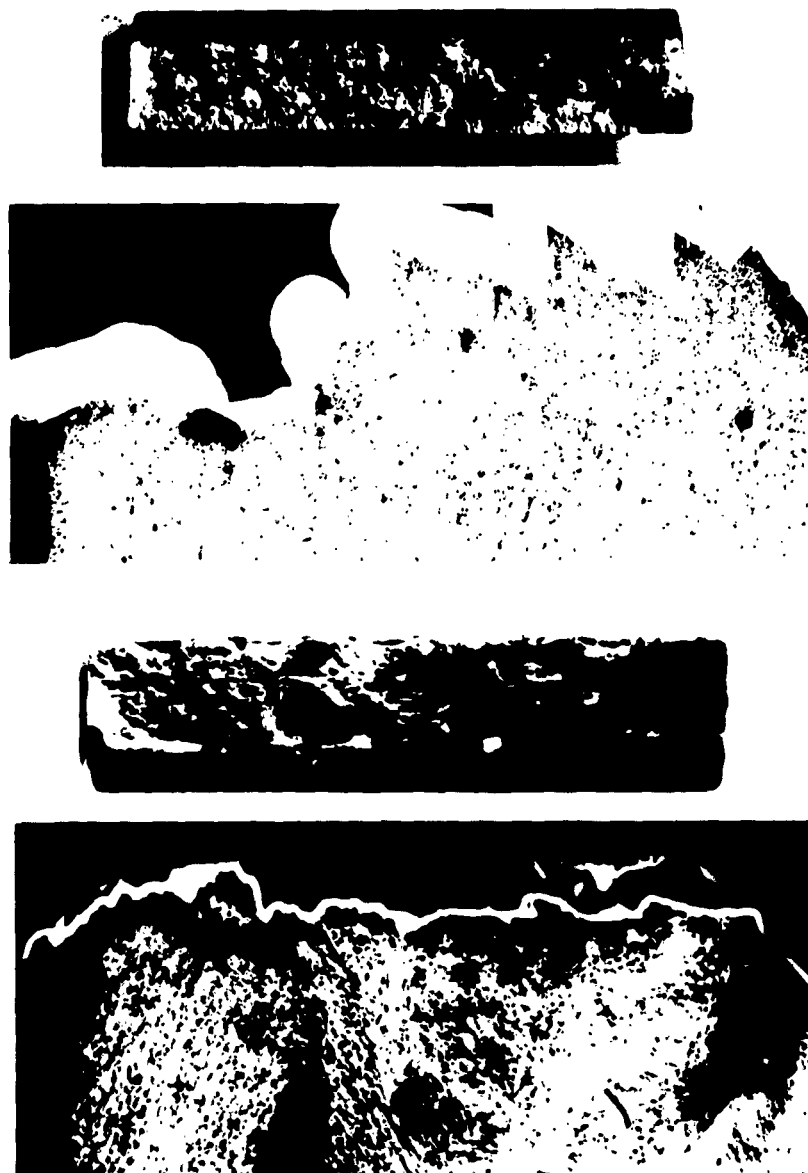
Figure II-14 - Top: Sample K, Austenitized at 1550°F, Tempered at 400°F, Broken at 70°F

Bottom: Sample V, Austenitized at 2300°F, Tempered at 400°F, Broken at 70°F

Magnifications: Sections, 50X; Fracture Surfaces, 7X
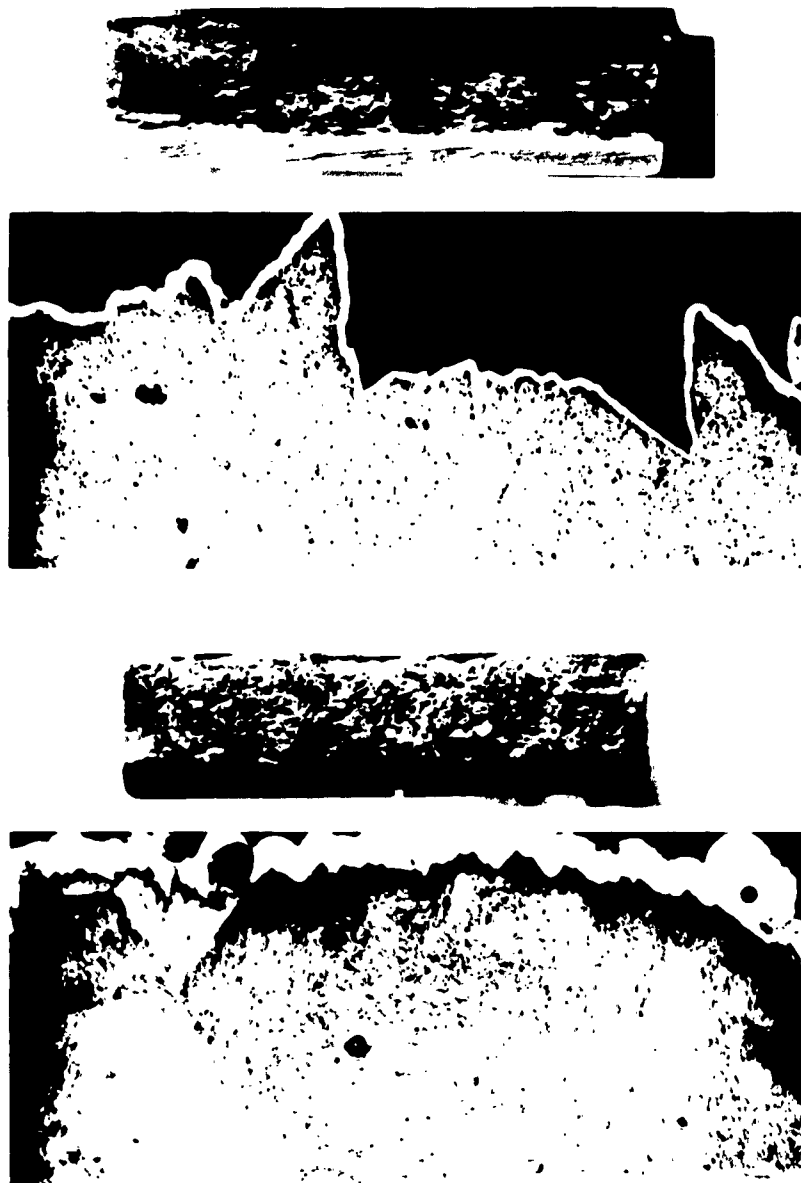
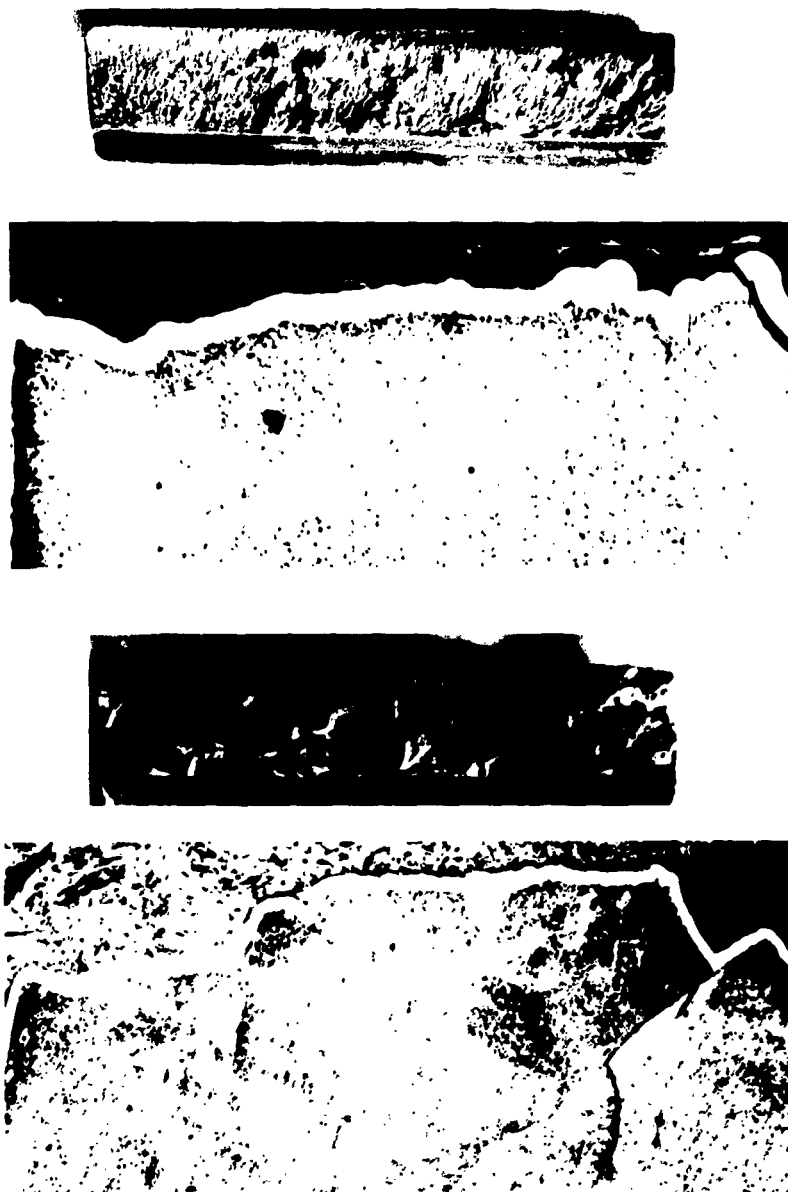Figure II-15 - Top: Sample F, Austenitized at 1550°F, Tempered at
                        400°F, Broken at 212°F

                Bottom: Sample BBB, Austenitized at 2300°F, Tempered at
                        400°F, Broken at 212°F

                Magnifications: Sections, 50X; Fracture Surfaces, 7X
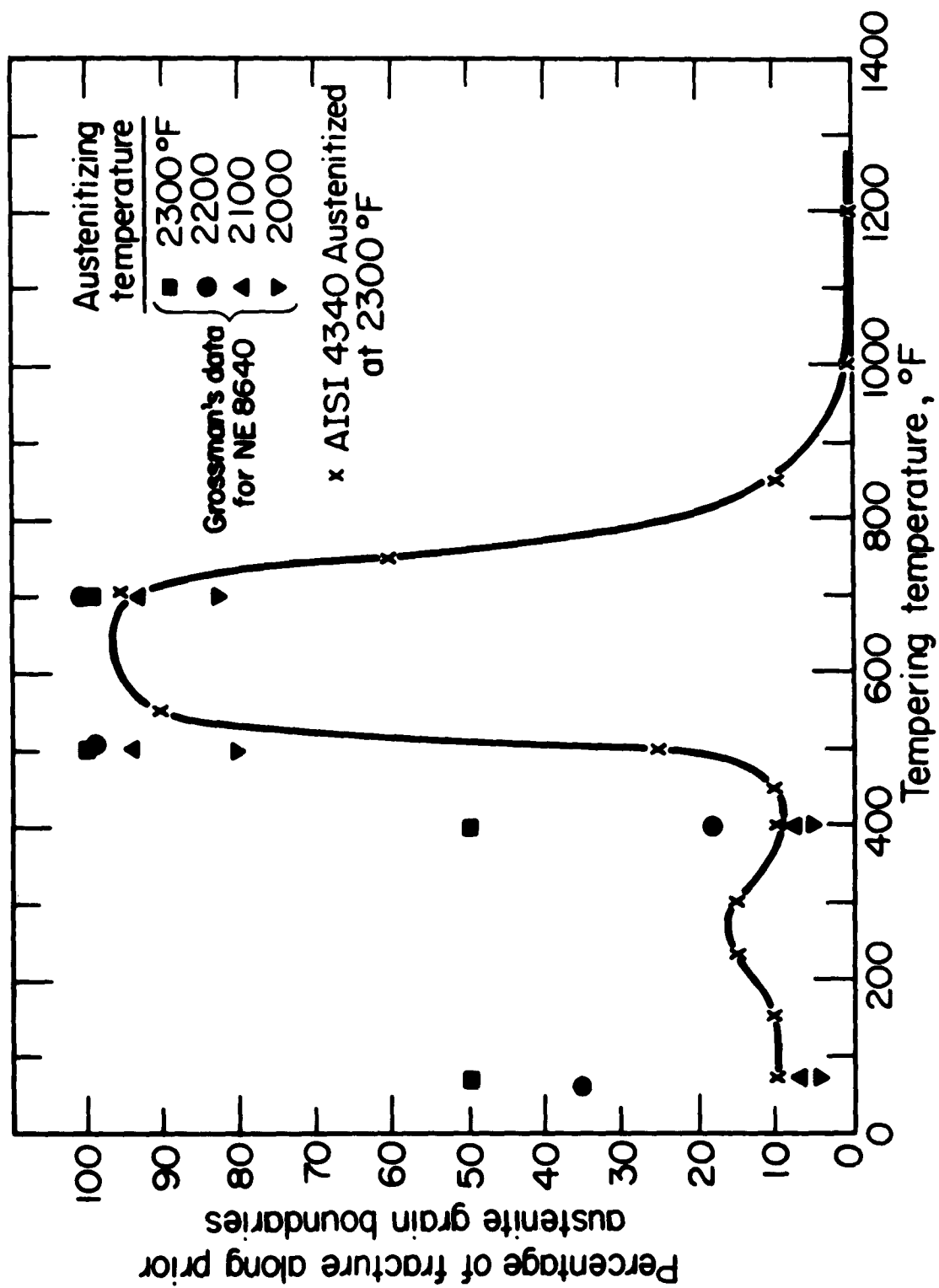
Figure II-16 – Percentage of Fracture along Prior Austenite Grain Boundaries for Specimens Tempered at Various Temperatures.
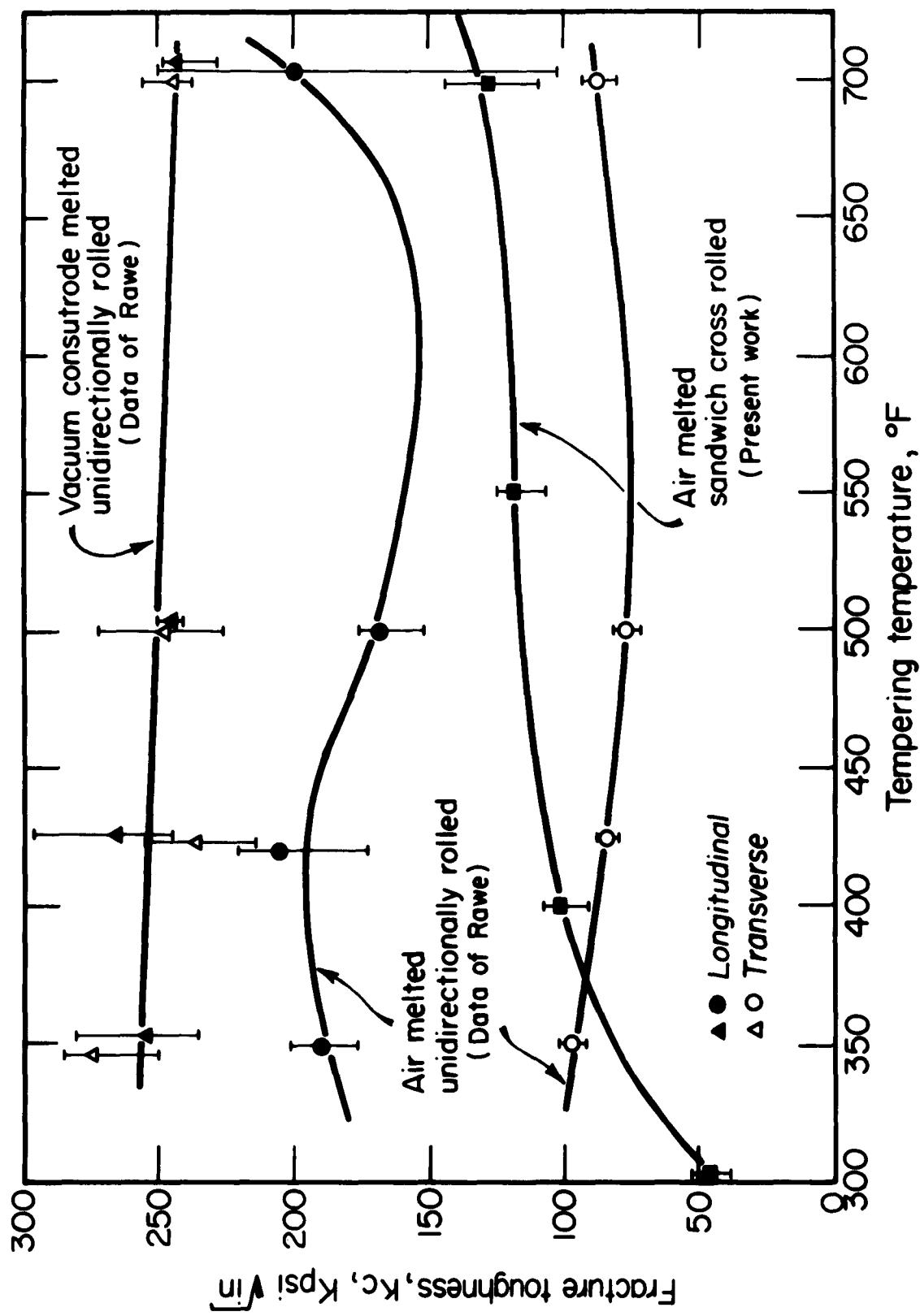
Figure I-17 — Effect of Processing History on K_c for AISI 4340. Data of Rawe from Ref. 5.

Testing Temperature: The surface roughness of specimens hardened from 1550°F and tempered at 400°F drops markedly as the testing temperature is lowered from 70 to -346°F (Figs. II-12 to II-15 top). The implied drop in fracture toughness is reasonable. Srawley and Beachem,[7] for example, have shown that K_c of 0.063 in. thick air-melted AMS 6434 steel quenched from 1600°F and tempered one hour at 400°F drops from 94 kpsi (in.)$^{1/2}$ at 0°F to 62 kpsi (in.)$^{1/2}$ at -110°F.

The fracture of all specimens quenched from 2300°F and tempered at 400°F were ductile when tested at down to -346°F (Figs. II-12 to II-16 bottom). The amount of grain-boundary fracture was small (less than 10%) and independent of testing temperature. No cleavage could be observed, even at the lowest test temperature (-346°F, Fig. II-12 bottom). As judged from the more extensive and uniform surface roughness, it might be expected that fracture toughness of coarse-grained material would be greater at all testing temperatures and the toughness transition temperature would be lower.

Recent work by Katz[8] gives some indication that such predictions made on the basis of fracture appearance may be confirmed with plane-strain toughness values (G_{IC}) of AISI 4340 rod. Katz compared G_{IC} as measured with circumferentially notched specimens (0.001 in. radius) austenitized at 1550 and 2300°F, refrigerated, and tempered at 400°F. Values after austenitizing at 2300°F were 251 and 114 in lb./in.^{2} at 70 and -238°F, respectively, while the comparable values for the lower austenitizing temperature were 79 and 47 in.-lb./in.^{2}.

IV. DISCUSSION

The results obtained thus far in the program lead to a conclusion not in accord with more traditional views: if intergranular fracture can be avoided, austenitizing at higher temperatures may prove to be a method for substantially increasing fracture toughness. However, the basis for disagreement with such a finding appears largely in earlier work on essentially plain-carbon steel. It has been demonstrated by Scott,[9] Schane,[10] Rolf[11] and Zackay,[12] for example, that medium-carbon steels, such as SAE 1040, do in fact have much poorer mechanical properties, the coarser the prior austenite grain size. Bullens[13] has pointed out that the tendency for the formation of a connected proeutectoid ferrite network is greater in coarse-grained as contrasted to fine-grained medium-carbon steels. Grossman[5] has made clear the adverse effect of such a ferrite network on notch properties of quenched and tempered steel. Thus it seems that in steels of SAE 1040 type the morphology of proeutectoid ferrite contributes importantly to the adverse effect of larger prior austenite grain size on mechanical properties.

Davenport and Bain[14] have also shown that increasing prior austenite grain size has an adverse effect on mechanical properties in an approximately eutectoid carbon steel after water quenching to martensite and tempering to R_c 50. Since network formation is unlikely in this composition, the results establish an effect of prior austenite grain size per se on properties. Although no data were available at the time relating to the effect of austenite

grain size on the mechanical properties of low alloy steels, Davenport and Bain did point out that "inherently fine-grained" and "inherently coarse-grained" steels may differ in their response to grain coarsening. In particular, they suggested that an inherently fine-grained steel, when coarsened, might lead to a finer martensite, as martensite is nucleated within the austenite grain. This behavior would not be expected in carbon steels, as Zackay[12] has shown that in this material the martensite plate size closely follows that of the prior austenite grain-diameter. While such an observation may or may not be relevant to increased toughness with higher austenitizing temperature, it does suggest that the mechanical properties of carbon steels and low alloy steels may differ in their relationship to grain size.

The question also remains as to whether the thermal treatment or the grain size it produces elevates toughness. The observation that the fracture after hardening from 2300°F evidences little delamination, whereas that after hardening from 1550°F shows marked delamination, suggests that considerable reshaping of the inclusion and segregation structure occurs at the higher austenitizing temperature. These structural changes could have marked effects on ductility, independent of the austenite grain size.

Avoiding intergranular fracture when heating to high austenitizing temperatures can be difficult in AISI 4340. Heating this steel above about 2200°F introduces the possibility of "overheating", a phenomenon characterized by the tendency to fracture along the austenite boundaries produced in the overheating range.[15] Such a structural deterioration has long been recognized, but it is not yet understood. Haworth and Christian[15] point out that the actual overheating temperature for AISI 4340 is quite variable, and considerable difference occurs from heat to heat even though produced according to the same practice. The relationship of austenitizing temperature, "overheating", and resulting microstructures is a subject of direct interest in the continuing program.

V. SUMMARY

1. The appearance of fractured face-notched specimens and two preliminary K_c measurements at room temperature indicate that the AISI 4340 under study is tougher when austenitized at 2300°F than at 1550°F.

2. Based on fracture appearance, the fracture toughness of coarse-grained AISI 4340 sheet initially remains constant or drops slightly and then increases with increasing tempering temperature.

3. The appearance of fracture in face-notched specimens suggests that the toughness transition temperature for hardened AISI 4340 sheet tempered at 400°F is lower for coarse-grained than for fine-grained material.

VI. REFERENCES

1. C. H. Shih, B. L. Averbach and M. Cohen, Trans. ASM 48 (1956), p. 86.

2. D. K. Bullens, Steel and Its Heat Treatment, Vol. I, John Wiley New York (1948), p. 349.

3. M. S. Grossman, Trans. AIME, 167, (1946), p. 39.

4. M. Baeyerts, E. S. Bumps and J. P. Sheehan, Armour Research Foundation TR No. 36 on ONR Contract N6 onr 274T01, Project NR 031-115, June 16, 1952.

5. B. S. Lement, B. L. Averbach and M. Cohen, Trans. ASM 46, (1954), p. 851.

6. A. M. Turkalo, Trans. AIME, 218 (1960), p. 24.

7. J. E. Srawley and C. D. Beacham, NRL Report 5507, Jan. 10, 1959.

8. R. N. Katz, WAL TN 320.1/8, Dec. 1961.

9. H. Scott, Trans. ASM 40, (1948), p. 775.

10. P. Schane, Jr., Trans. ASM, 22, (1934), p. 1038.

11. R. L. Rolf, Heat Treating Forging, .° (1.°.), p. °/1, °31.

12. V. F. Zackay, ASM Seminar, Strengthening Mechanism of Solids, October (1960), in press.

13. Bullens, op. cit., p. 347.

14. E. S. Davenport and E. C. Bain, Trans. ASM 22, (1934), p. 879.

15. R. D. Haworth, Jr. and A. F. Christian, Proc. ASTM 45, (1945), p. 407.

ACKNOWLEDGEMENTS

DISTRIBUTION LIST

(Tasks A, B, C & D, 5010.11.843)   No. of Copies

A.   Department of Defense

Office of the Director of Defense Research & Engineering
ATTN: Mr. J. C. Barrett
Room 3D-1067, The Pentagon
Washington 25, D. C.   1

Advanced Research Project Agency
ATTN: Dr. G. Mock
The Pentagon
Washington 25, D. C.   1

Commander
Armed Services Technical Information Agency
ATTN: TIPDR
Arlington Hall Station
Arlington 12, Virginia   10

Defense Metals Information Center
Battelle Memorial Institute
Columbus, Ohio   1

Solid Propellant Information Agency
Applied Physics Laboratory
The Johns Hopkins University
Silver Spring, Maryland   3

B.   Department of the Army - Technical Services

Office Chief of Ordnance
ATTN: ORDTB-Materials
Department of the Army
Washington 25, D. C.   1

Commanding General
Aberdeen Proving Ground
ATTN: Dr. C. Pickett, C&CL
Aberdeen Proving Ground, Maryland   1

Commanding General
Ordnance Tank-Automotive Command
ATTN: Mr. S. Sobak, ORDMC-IF-2
Detroit 9, Michigan   1

DISTRIBUTION LIST

(Tasks A, B, C & D, 5010.11.843)   <u>No. of Copies</u>

Commanding General
Ordnance Weapons Command
ATTN: Mr. B. Gerke, ORDOW-IA
Rock Island, Illinois   1

Commanding General
U.S. Army Ballistic Missile Agency
ATTN: Dr. G. H. Reisig   1
       Mr. P. B. Wallace, ORDAB-RPEM   1
       Documentaion & Technical Information Branch   2
       ORDAB-IEE   1
Redstone Arsenal, Alabama   1

Commanding General
U.S. Army Rocket & Guided Missile Agency
ATTN: Mr. Robert Fink, ORDXR-RGS   1
       Mr. W. H. Thomas, ORDXR-IQI   1
Redstone Arsenal, Alabama

Commanding Officer
Frankford Arsenal
ATTN: Dr. H. Gisser, ORDBA-1330   1
       Mr. H. Markus, ORDBA-1320   1
Philadelphia 37, Pa.

Commanding Officer
Ordnance Materials Research Office
Watertown Arsenal
ATTN: RPD
Watertown 72, Mass.   1

Commanding Officer
Picatinny Arsenal
ATTN: Mr. J. J. Scavuzzo, Plastics & Packaging Lab.   3
       Mr. D. Stein, ORDBB-DE3   1
Dover, N. J.

Commanding Officer
PLASTEC
Picatinny Arsenal
Dover, N. J.   1

Commanding Officer
Rock Island Arsenal
ATTN: Materials Section, Laboratory
Rock Island, Illinois   1

DISTRIBUTION LIST

(Tasks A, B, C & C, 5010.11.843)   No. of Copies

Commanding Officer
Springfield Armory
ATTN: Mr. R. Korytoski, Research Materials Lab.
Springfield 1, Mass.   1

Commanding Officer
Watertown Arsenal
ATTN: ORDBE-LX
Watertown 72, Mass.   3

Commanding Officer
Watervliet Arsenal
ATTN: Mr. F. Dashnaw, ORDBF-RR
Watervliet, New York   1

Headquarters
U.S. Army Signal R&D Laboratory
ATTN: Mr. H. H. Kedsky, SIGRA/SL-XE
Fort Monmouth, N. J.   1

Department of the Army - Other Army Agencies

Commander
Army Research Office
Arlington Hall Station
Arlington 12, Virginia   1

Chief of Research and Development
U.S. Army Research and Development Liaison Group
ATTN, Dr. B. Stein
APO 757, New York, N. Y.   1

C. Department of the Navy

Chief, Bureau of Naval Weapons
Department of the Navy
ATTN: RMMP
Room 2225, Munitions Building
Washington 25, D. C.   1

Department of the Navy
Office of Naval Research
ATTN: Code 423
Washington 25, D. C.   1

DISTRIBUTION LIST

(Tasks, A, B, C & D, 5010.11.843)   <u>No. of Copies</u>

Department of the Navy
Special Projects Office
ATTN: SP 271
Washington 25, D. C.   1

Commander
U.S. Naval Ordnance Laboratory
ATTN: Code WM
White Oak, Silver Spring, Maryland   1

Commander
U.S. Naval Ordnance Test Station
ATTN: Technical Library Branch
China Lake, California   1

Commander
U.S. Naval Research Laboratory
ATTN: Mr. J. E. Srawley
Anacostia Station
Washington 25, D. C.   1

D. <u>Department of the Air Force</u>

U.S. Air Force Directorate of Research & Development
ATTN: Lt. Col. J. B. Shipp, Jr.
Room 4D-313, The Pentagon
Washington 25, D. C.   1

Wright Air Development Division
ATTN: H. Zoeller, ASRCEE-1
Wright-Patterson Air Force Base, Ohio   2

ARDC Flight Test Center
ATTN: Solid Systems Division, FTRSC
Edwards Air Force Base, California   5

AMC Aeronautical Systems Center
ATTN: Manufacturing & Materials Technology Div, LMBMO
Wright Patterson Air Force Base, Ohio   2

DISTRIBUTION LIST

(Tasks, A, B, C & D, 5010.11.843)   No. of Copies

E. **Other Government Agencies**

National Aeronautics and Space Administration
ATTN: Mr. R. V. Rhode   1
        Mr. G. C. Deutch   1
Washington D. C.

Dr. W. Lucas
George C. Marshall Space Flight Center
National Aeronautics and Space Administration
ATTN: M-S&M-M
Huntsville, Alabama   1

Dr. L. Jaffe
Jet Propulsion Laboratory
California Institute of Technology
4800 Oak Grove Drive
Pasadena, California   1

Mr. William A. Wilson
George C. Marshall Space Flight Center
ATTN: M-F&AE-M
Huntsville, Alabama   1

F. **Defense Contractors**

Aerojet-General Corporation
ATTN: Librarian
Post Office Box 1168
Sacramento, California   1

Aerojet-General Corporation
ATTN: Librarian   1
       Mr. C. A. Fournier   1
Post Office Box 296
Azusa, California

Allison Division
General Motors Corporation
ATTN: Mr. D. K. Hanink
Indianapolis 6, Indiana   1

DISTRIBUTION LIST

(Tasks, A, B, C & D, 5010.11.843)   <u>No. of Copies</u>

ARDE-Portland, Inc.
ATTN: Mr. R. Alper
100 Century Road
Paramus, N. J.   1

Atlantic Research Corporation
ATTN: Mr. E. A. Olcott
Shirley Highway and Edsall Road
Alexandria, Virginia   1

Curtiss-Wright Corporation
Wright Aeronautical Division
ATTN: Mr. R. S. Shuris   1
       Mr. A. M. Kettle, Technical Library   1
Wood-Ridge, N. J.

Hercules Powder Company
Allegheny Ballistics Laboratory
ATTN: Dr. R. Steinberger
Post Office Box 210
Cumberland, Maryland   1

Hughes Aircraft Company
ATTN: Librarian
Culver City, California   1

Tapco Group
ATTN: Mr. W. J. Piper
23555 Euclid Avenue
Cleveland 17, Ohio   1

SUPPLEMENTAL DISTRIBUTION LIST

(Task A, Case Matls. & Fabrication, 5010.11.843)　　　<u>No. of Copies</u>

A. <u>Department of the Navy</u>

Chief, Bureau of Naval Weapons
Department of the Navy
ATTN:　Mr. P. Goodwin
Washington 25, D. C.　　　　　　　　　　　　　　　　1

B. <u>Department of the Air Force</u>

Headquarters
Aeronautical Systems Division
ATTN:　Dr. Tamborski, ASRCNP
Wright-Patterson Air Force Base, Ohio　　　　　　　1

Wright Air Development Division
ATTN:　Mr. G. Peterson, ASRCNC-1
Wright-Patterson Air Force Base, Ohio　　　　　　　1

C. <u>Defense Contractors</u>

Allegheny Ludlum Steel Corporation
Research Center
ATTN:　Mr. R. A. Lula
Brackenridge, Pennsylvania　　　　　　　　　　　　1

Alloyd Electronics-Corporation
ATTN:　Dr. S. S. White
35 Cambridge Parkway
Cambridge, Mass.　　　　　　　　　　　　　　　　1

Armco Steel Corporation
General Offices
ATTN:　Mr. J. Barnett
Middletown, Ohio　　　　　　　　　　　　　　　　1

Battelle Memorial Institute
ATTN:　Mr. R. Monroe　　　　　　　　　　　　　　1
　　　　Mr. G. Faulkner　　　　　　　　　　　　　1
505 King Avenue
Columbus 1, Ohio

SUPPLEMENTAL DISTRIBUTION LIST

(Task A, Case Matls. & Fabrication, 5010.11.843)   <u>No. of Copies</u>

The Boeing Company
Aero Space Division
P. O. Box 3707
Seattle 24, Washington   1

Borg-Warner Corporation
Ingersoll Kalamazoo Division
ATTN: Mr. L. E. Hershey
1810 N. Pitcher St.
Kalamazoo, Michigan   1

The Budd Company
Defense Division
ATTN: Mr. R. C. Dethloff   1
      Mr. Ohman   1
Philadelphia 32, Pennsylvania

Climax Molybdenum Company
ATTN: Mr. R. R. Freeman
1270 Avenue of the Americas
New York 20, N. Y.   1

Douglas Aircraft Company Inc.
Santa Monica Division
ATTN: Mr. J. L. Waisman
Santa Monica, California   1

General Electric Company
Rocket Engine Section
Flight Propulsion Laboratory Department
Cincinnati 15, Ohio   1

Jones and Laughlin Steel Corporation
ATTN: Mr. H. Steinbrenner
45 South Montgomery Avenue
Youngstown 1, Ohio   1

Arthur D. Little, Inc.
ATTN: Dr. R. Davis
Acorn Park
Cambridge 40, Mass.   1

SUPPLEMENTAL DISTRIBUTION LIST

(Task A, Case Matls. & Fabrication, 5010.11.843)   **No. of Copies**

Lyon, Inc.
ATTN: Mr. W. Martin
13881 W. Chicago Boulevard
Detroit, Michigan   1

Manufacturing Laboratories
ATTN: Dr. P. Fopiano   1
      Dr. V. Radcliffe   1
21-35 Erie Street
Cambridge 42, Mass.

Minneapolis-Honeywell Regulator Company
1230 Soldiers Field Road
Boston 35, Mass.   1

Norris-Thermador Corporation
ATTN: Mr. L. Shiller
5215 South Boyle Avenue
Los Angeles 58, California   1

The Perkin-Elmer Corporation
ATTN: Mr. H. L. Sachs
Main Avenue
Norwalk, Connecticut   1

Pratt & Whitney Aircraft
ATTN: Mr. F. A. Crosby
East Hartford, Connecticut   1

Reactive Metals Corporation
ATTN: Mr. H. Lundstrom
Niles, Ohio   1

Republic Steel Corporation
Research Center
ATTN: Mr. H. P. Manger
Independence, Ohio   1

Rohm & Haas Company
Redstone Arsenal Research Division
ATTN: Library
Huntsville, Alabama   1

SUPPLEMENTAL DISTRIBUTION LIST

(Task A, Case Matls. & Fabrication, 5010.11.843)   No. of Copies

Space Technology Laboratories, Inc.
ATTN: Technical Information Center Document Procurement
Post Office Box 95001
Los Angeles 45, California   1

Thiokol Chemical Corporation
Utah Division
Brigham City, Utah   1

Titanium Metals Corporation
ATTN: Mr. G. Erbin
233 Broadway
New York, N. Y.   1

Universal-Cyclops Steel Corp.
Stewart Street
Bridgeville, Pennsylvania   1

U.S. Borax Research Corp.
ATTN: Mr. R. J. Brotherton
412 Crescent Way
Anaheim, California   1

United States Rubber Company
Research Center
ATTN: Dr. E. J. Joss
Wayne, N. J.   1

D. Educational Institutions

Mellon Institute
ATTN: Dr. H. L. Anthony   1
       Mr. C. J. Owen   1
4400 Fifth Avenue
Pittsburgh 13, Pa.

Michigan State University
ATTN: Mr. R. N. Hammer
Department of Chemistry
East Lansing, Michigan   1

SUPPLEMENTAL DISTRIBUTION LIST

(Task A, Case Matls. & Fabrication, 5010.11.843)   No. of Copies

Ohio State University
Research Foundation
ATTN: Dr. R. McMaster
Columbus, Ohio   1

E. Commanding Officer
Boston Ordnance District
ATTN: Contracting Officer's Rep., ORDEB LD
Boston Army Base
Boston 10, Massachusetts   1